Chapter 22 Fractal Neuronal Firing Patterns

MALVIN C. TEICH
Department of Electrical Engineering
Columbia University
New York, New York

I. Introduction

The sequence of action potentials produced by a neuron is best characterized in terms of a stochastic point process (Teich, 1989; Teich and Khanna, 1985). This is because the information is encoded in the occurrence times, rather than in the magnitudes, of the unitary neural events, and these occurrence times are random. The mathematical process that has been traditionally used in auditory, and other branches, of sensory neurophysiology has been the *dead-time-modified Poisson point process,* denoted DTMP (Gaumond *et al.,* 1982; Gray, 1967; Kuffler *et al.,* 1957; Mueller, 1954; Prucnal and Teich, 1983; Teich *et al.,* 1978; Young and Barta, 1986). Theoretical results for the DTMP process are widely available in the literature (Cox, 1962; Müller, 1974; Prucnal and Teich, 1983; Ricciardi and Esposito, 1966; Teich, 1985). This model of neuronal firing achieved its principal successes in describing *interspike-interval histograms* (or pulse-interval distributions, PIDs) and *post-stimulus-time histograms* (PSTs), measures that reset at relatively short times and are therefore insensitive to long-time correlations in spike occurrences. The predictions of the DTMP model turn out to be at odds with many other observed statistical measures of neurophysiological data. In particular, it is now quite clear that the DTMP fails to provide a proper characterization of the sequence of action potentials in the auditory neurons of a number of species (Teich *et al.,* 1990a).

Auditory signals transmitted from the hair-cell receptor in the cochlea to the

M. C. Teich, "Fractal Neuronal Firing Patterns," in Single Neuron Computation, edited by T. McKenna, J. Davis, and S. F. Zornetzer (Academic Press, Boston, 1992), ch. 22, pp. 589-625

cortex (and beyond) pass through many way stations located along the auditory pathways. In recent years, the responses of receptor cells, as well as the primary auditory-nerve-fiber neurons that attach to them, have been studied in great detail in many species, both in the presence and in the absence of various kinds of acoustic stimulation. The *patterns* of neuronal firing have been examined in single mammalian neurons at various locations along this pathway, including the auditory nerve (AN), the cochlear nucleus (CN), which is the first way station, and the lateral superior olivary complex (LSO).

The sequences of action potentials observed from single neurons at the AN, CN, and LSO turn out to exhibit long-term correlations that are not captured in the interspike-interval and post-stimulus-time histograms (Teich, 1989; Teich and Khanna, 1985). The properties of these spike trains are unusual. They manifest highly irregular spike rates, even when the integration time is very long; broad pulse-number distributions (which are histograms of the relative frequency of observing a given number of spikes versus the spike number); fractional power-law growth of the variance-to-mean ratio with the counting time T (Fano-factor time curve) with an exponent that depends on the level of stimulation; and $1/f$-type behavior in the spectrum (Teich, 1989; Teich *et al.*, 1990a, b; Woo *et al.*, 1992a).

The firing patterns of these neurons are characterized as *fractal* because the spike-rate fluctuations are self-similar over a large range of integration times. This self-similarity is also evident in the spectrum. These properties bespeak correlation that decays in power-law fashion, and therefore long-term memory, at the periphery of the auditory system.

Fractal patterns exhibit order within apparent randomness, and reveal the presence of multiple scales of time and/or space. All primary auditory neurons examined to date, both in the presence and in the absence of an acoustic stimulus, exhibit this behavior for sufficiently large observation times, as has now been confirmed in cat and chinchilla in a number of laboratories (Powers, 1991; Powers *et al.*, 1991; Teich *et al.*, 1990b; Woo, 1991; Woo *et al.*, 1992). Fractal behavior also appears to be present at the CN (Shofner and Dye, 1989) and may be present at the LSO (Turcott *et al.*, 1991).

In contrast to this behavior, the patterns associated with primary vestibular neurons have not been found to exhibit long-term correlations and appear to be non-fractal (Teich, 1989). It may be that fractal neural firings in the auditory

FIGURE 1. (a) Spontaneous firing rate of a primary auditory neuron (unit A, CF = 10.2 kHz). Two different time windows were used to compute the rate: $T = 0.5$ s (solid curve) and $T = 5.0$ s (dashed curve). (b) The firing rate of a simulated dead-time-modified Poisson (DTMP) point process with the same time windows. From Teich *et al.* (1990b).

M. C. Teich, "Fractal Neuronal Firing Patterns," in Single Neuron Computation, edited by T. McKenna, J. Davis, and S. F. Zornetzer (Academic Press, Boston, 1992), ch. 22, pp. 589-625

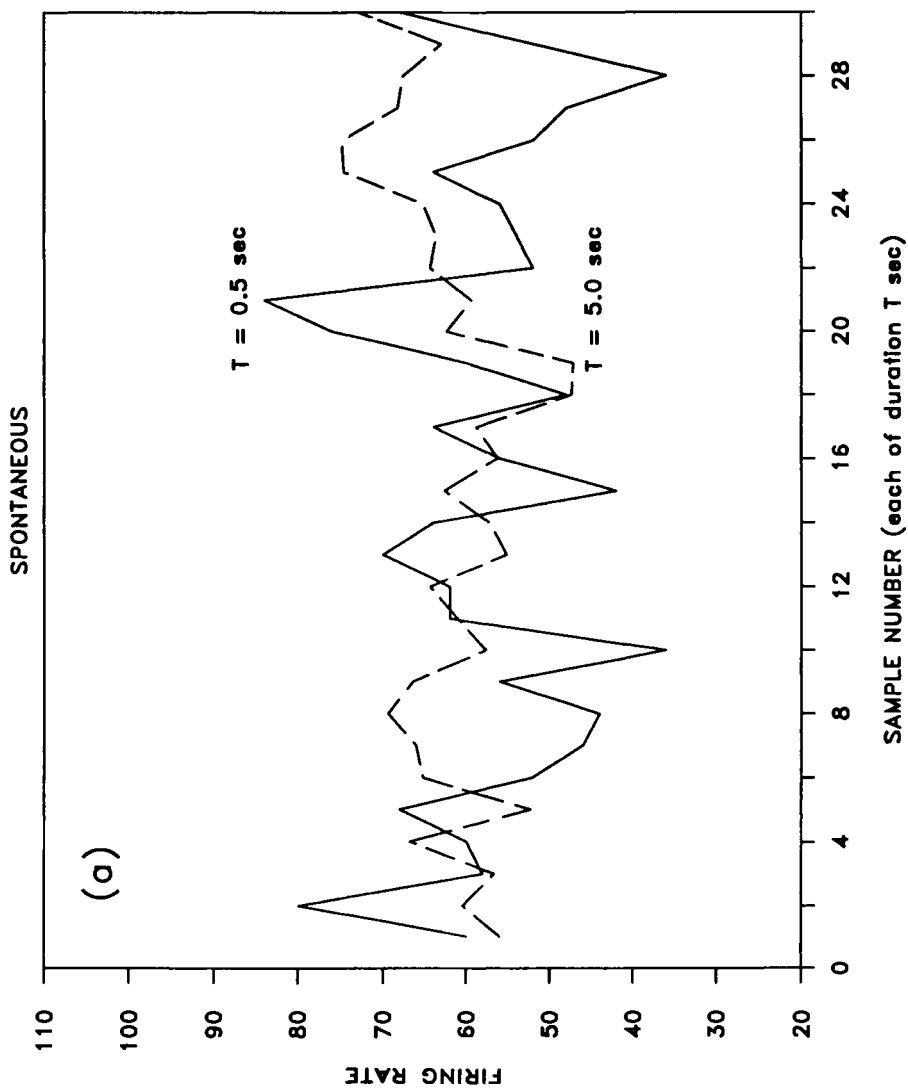

M. C. Teich, "Fractal Neuronal Firing Patterns," in Single Neuron Computation, edited by T. McKenna, J. Davis, and S. F. Zornetzer (Academic Press, Boston, 1992), ch. 22, pp. 589-625

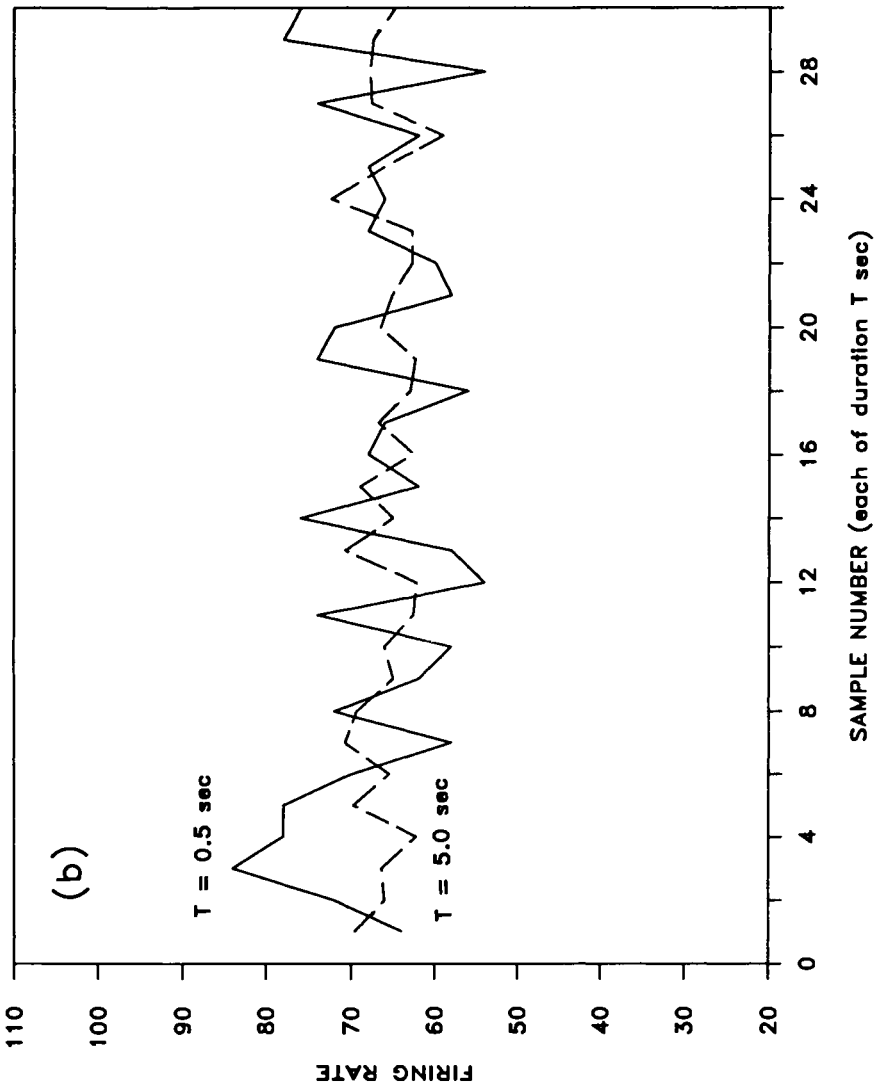

FIGURE 1. *Continued*

M. C. Teich, "Fractal Neuronal Firing Patterns," in Single Neuron Computation, edited by T. McKenna, J. Davis, and S. F. Zornetzer (Academic Press, Boston, 1992), ch. 22, pp. 589-625

system serve to provide efficient sampling of natural fractal sounds. Several biophysical mechanisms present themselves as possible origins of this behavior, as discussed later in this chapter.

In seeking to identify the point process that properly models auditory neural firings, we have constructed a doubly stochastic Poisson point process (DSPP) driven by fractal shot noise (FSN), abbreviated FDSPP, or FSNDP (Lowen and Teich, 1990, 1991). With the incorporation of dead-time effects (absolute refractoriness) and/or sick-time effects (relative refractoriness), this process appears to work remarkably well in describing the fractal firing patterns of primary auditory-nerve neurons, both in the presence of a pure-tone stimulus and in its absence (spontaneous firings) (Teich *et al.*, 1990a).

II. Self-Similarity of Neuronal Firing Rates

Perhaps the simplest measure of a sequence of action potentials is its rate, i.e., the number of spikes registered per unit time. In primary auditory neurons, even this straightforward measure has unusual properties; the magnitude of the fluctuations of the rate does not decrease appreciably, even when a very long averaging period (time window) is used to compute the rate. This property reflects fractal behavior and is in direct opposition to the predictions of the DTMP process.

In Fig. 1a, we illustrate the firing rate of a spontaneously active adult-cat auditory neuron (unit A) with a characteristic frequency (CF) = 10.2 kHz. Two different time windows were used to compute the rate: $T = 0.5$ s (solid curve) and $T = 5.0$ s (dashed curve). The total time duration of the solid curve is 15 s (30 consecutive time windows, each of 0.5 s), whereas the total time duration of the dashed curve is 150 s (30 consecutive time windows, each of 5.0 s). Evidently, increasing the averaging time by a factor of 10 does not appreciably reduce the magnitude of the fluctuations.

The firing rate of a simulated DTMP point process is illustrated in Fig. 1b. The rate and time windows were chosen to be the same as those for the auditory data shown in Fig. 1a, and the (fixed, nonparalyzable) dead time was taken to be $\tau_d = 2.95$ ms (for reasons that will become apparent in Section III). The $T = 5.0$ s computer data (dashed curve) exhibits noticeably smaller fluctuations than does the $T = 0.5$ s computer data (solid curve). This smoothing with increased averaging time does not occur with the neural data.

The contrast is even more dramatic in the case of driven activity, as illustrated in Fig. 2a. Firing-rate data are shown for the same neuron as illustrated in Fig. 1a, but now with continuous-tone stimulation at the CF. The rate is generally

M. C. Teich, "Fractal Neuronal Firing Patterns," in Single Neuron Computation, edited by T. McKenna, J. Davis, and S. F. Zornetzer (Academic Press, Boston, 1992), ch. 22, pp. 589-625

higher than that in Fig. 1a because the neuron is driven. Three different time windows are used to compute the rate: $T = 0.5$ s (solid curve), $T = 5.0$ s (dashed curve), and $T = 50$ s (dotted curve). The total time duration of the solid curve is 15 s (30 consecutive time windows, each of 0.5 s), the total time duration of the dashed curve is 150 s (30 consecutive time windows, each of 5.0 s), and the total time duration of the dotted curve is 550 s (11 consecutive time windows, each of 50 s). To minimize the effects of nonstationarity arising from adaptation, the data presented in Fig. 2a begins 250 s after the onset of the stimulus. The fluctuations of the rate do not appear to be smoothed, even though the change of time scale is a factor of 100 (from $T = 0.5$ s to $T = 50$ s); the process may be said to be self-similar (Mandelbrot, 1983; Teich, 1989).

The firing rate of a simulated DTMP process with the same rate, but now with a dead time $\tau_d = 2.48$ ms, is illustrated in Fig. 2b for comparison. The time windows are the same as those used in Fig. 2a. The substantial smoothing of the rate fluctuations with increasing counting time is in dramatic contrast to the self-similar behavior apparent in the auditory data. This clearly shows that the DTMP is not a satisfactory model for the auditory data.

III. Power-Law Growth of the Spike-Number Variance-to-Mean Ratio

The *pulse-number distribution* (PND) is a commonly used characteristic of a point process. It is an estimate of the probability $p(n,T)$ of observing n spikes in the observation time T versus the number of spikes n. A useful statistic of the PND is provided by the spike-number (count) variance-to-mean ratio

$$F = \frac{\text{Var}(n)}{\langle n \rangle}. \tag{1}$$

FIGURE 2. (a) Firing rate of an auditory neuron (unit A, same cell as displayed in Fig. 1) driven by a continuous tone at the characteristic frequency. Three time windows were used to compute the rate: $T = 0.5$ s (solid curve), $T = 5.0$ s (dashed curve), and $T = 50$ s (dotted curve). Increasing the averaging time by a factor of 100 does not appreciably decrease the magnitude of the fluctuations; the continuous-tone-driven process is self-similar. (b) The firing rate of a simulated dead-time-modified Poisson point process with the same time windows as in a. The evident smoothing of the rate fluctuations with increasing counting time is in dramatic contrast to the self-similar behavior observed in the auditory data. From Teich *et al.* (1990b).

M. C. Teich, "Fractal Neuronal Firing Patterns," in Single Neuron Computation, edited by T. McKenna, J. Davis, and S. F. Zornetzer (Academic Press, Boston, 1992), ch. 22, pp. 589-625

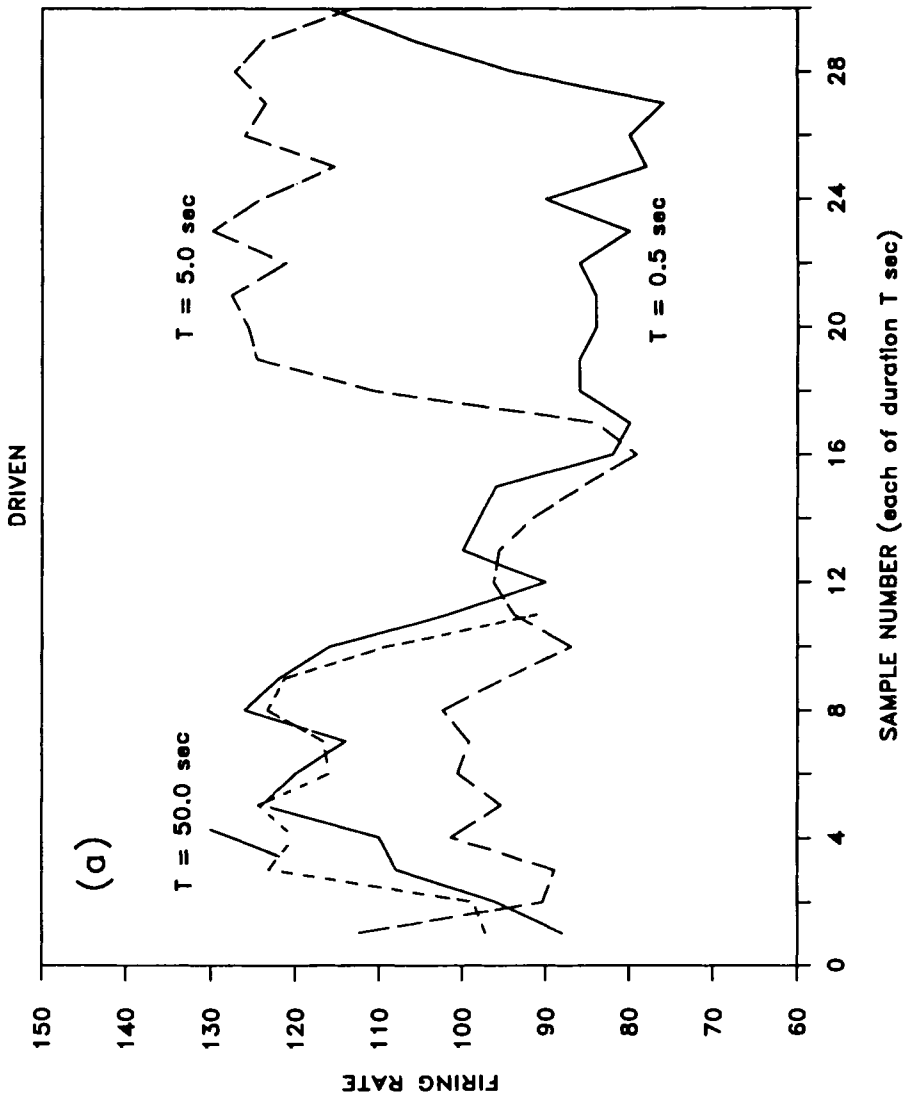

M. C. Teich, "Fractal Neuronal Firing Patterns," in Single Neuron Computation, edited by T. McKenna, J. Davis, and S. F. Zornetzer (Academic Press, Boston, 1992), ch. 22, pp. 589-625

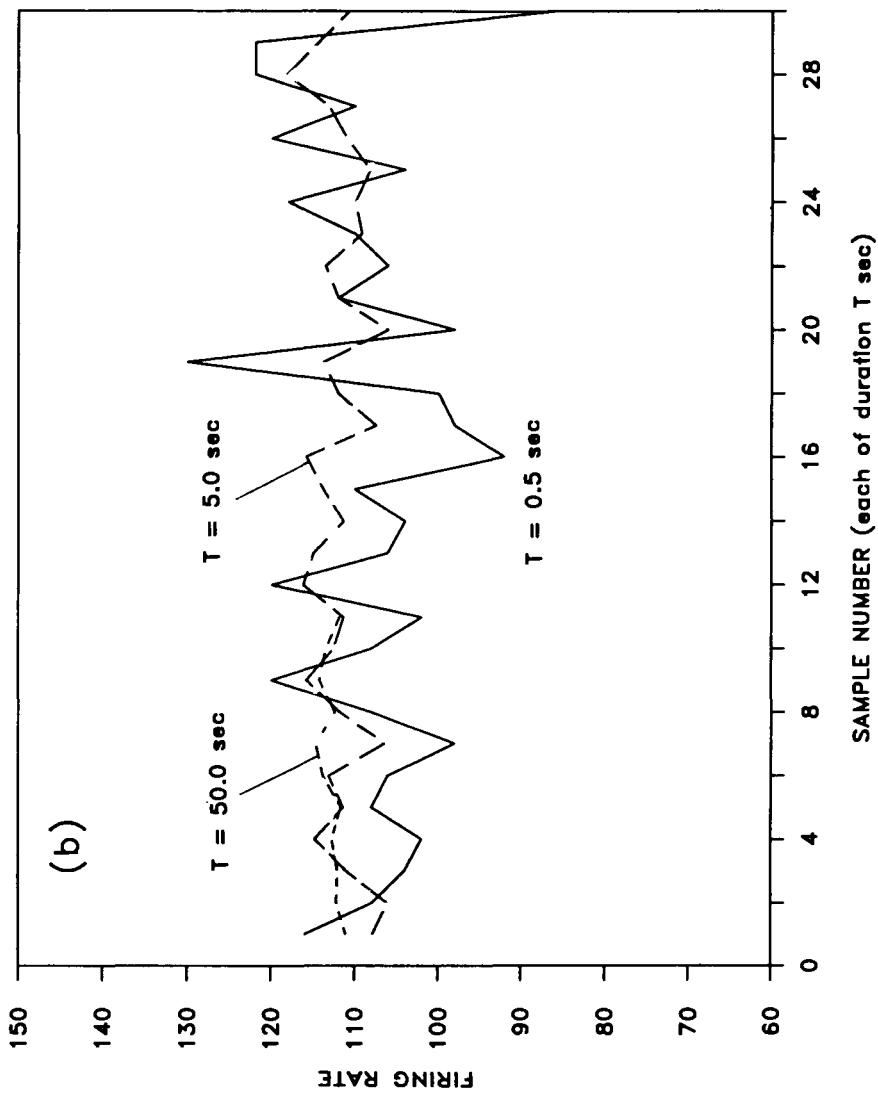

FIGURE 2. *Continued*

M. C. Teich, "Fractal Neuronal Firing Patterns," in Single Neuron Computation, edited by T. McKenna, J. Davis, and S. F. Zornetzer (Academic Press, Boston, 1992), ch. 22, pp. 589-625

This quantity is often referred to as the *Fano factor*, since it was first used by Fano (1947) as a measure of the statistical fluctuations of the number of ions generated by individual fast charged particles.

The *Fano-factor time curve* (FFC) is the ratio of the count variance to the count mean for different counting times T. It is designated $F(T)$, and is shown in Fig. 3 for unit A under conditions of spontaneous firing (dashed curve). This plot is obtained using the same spike train that provided the firing rates shown in Figs. 1a and 2a. (The spontaneous firing rate was about 60 s^{-1} and the overall duration of the experiment was $L = 400$ s.) The FFC is seen to assume a value of unity at short counting times, dip below unity for counting times above about 1 ms (where refractoriness comes into play), and finally to increase with T in power-law fashion (with an exponent $\alpha \approx 0.68$ for this particular neuron) when the counting time exceeds 400 ms. All primary auditory neurons examined exhibited this characteristic FFC shape. For spontaneous activity in the absence of a stimulus, F typically assumes a minimum value F_{min} between about 0.6 and 1.0 at counting times in the tens of ms. The onset of pure power-law behavior (with exponents in the range between about 0.3 and 0.9) occurs at counting times between about 0.1 and 1.0 s. The fractal nature of the process manifests itself in the power-law regime.

The FFC for a simulated dead-time-modified Poisson process (DTMP) is shown for comparison (solid curve). It assumes a value of unity when $T \ll \tau_d$ (as expected for a Bernoulli process with low probability of success), dips below unity when the counting time T approaches τ_d, and remains approximately constant, at a value below unity, for all values of $T \gg \tau_d$. The asymptotic value assumed by the DTMP Fano factor F_d for counting times large in comparison with the dead time is (Teich, 1985):

$$F_d \approx (1 - \lambda\tau_d)^2, \tag{2}$$

where λ represents the post-dead-time firing rate. The minimum value of the Fano factor observed for unit A, $F_d \approx 0.68$, requires $\tau_d = 2.95$ ms, since $\lambda = 60$ s^{-1}. The dead-time simulations exhibited in Figs. 3, 1b, and 2b all make use of values of τ_d that satisfy Eq. (2) when the observed values of λ and F_{min} are used.

Poisson processes modified by stochastic dead time or by sick time, which are physiologically more realistic, lead to Fano-factor time curves similar to those for fixed dead time (Teich and Diament, 1980; Teich *et al.*, 1978; Young and Barta, 1986). The fixed dead-time approximation is usually adequate when considering count (as opposed to interval) measures of the spike train.

M. C. Teich, "Fractal Neuronal Firing Patterns," in Single Neuron Computation, edited by T. McKenna, J. Davis, and S. F. Zornetzer (Academic Press, Boston, 1992), ch. 22, pp. 589-625

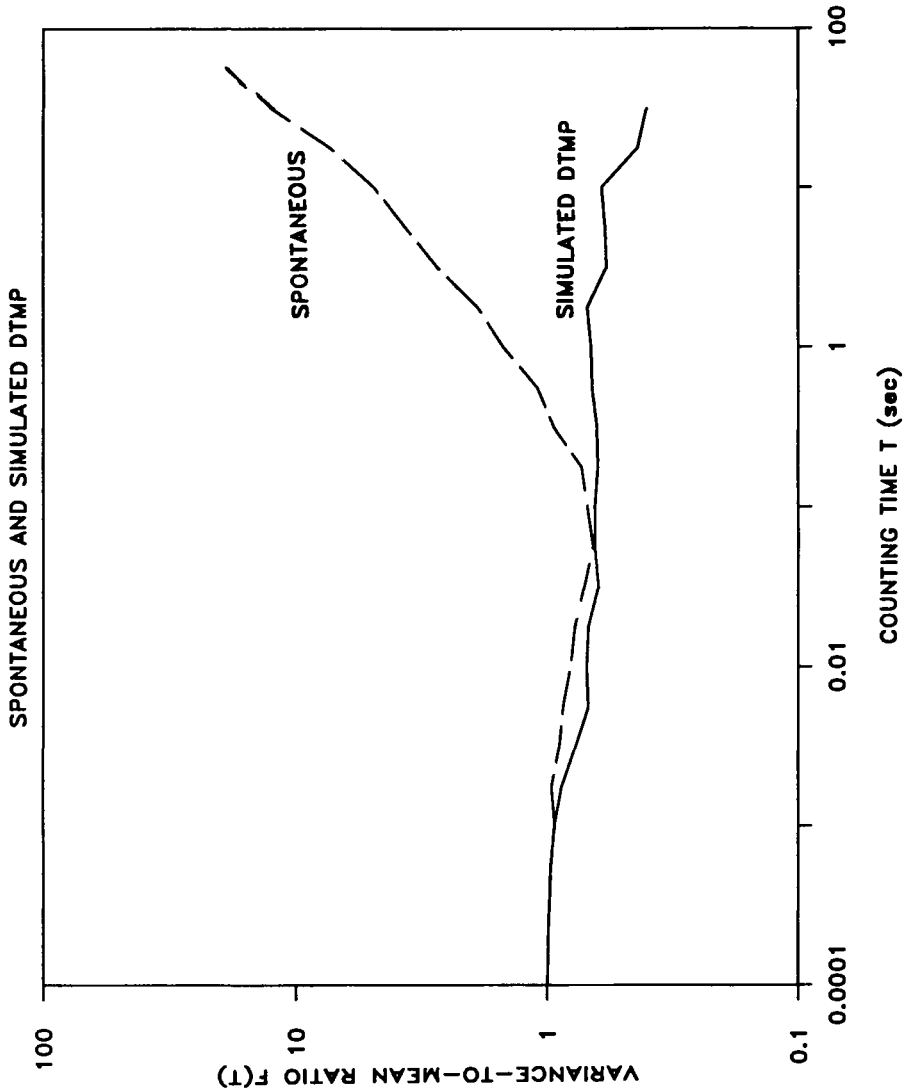

M. C. Teich, "Fractal Neuronal Firing Patterns," in Single Neuron Computation, edited by T. McKenna, J. Davis, and S. F. Zornetzer (Academic Press, Boston, 1992), ch. 22, pp. 589-625

IV. Fractal Dimension of the Firing Pattern

The fractal dimension of the firing pattern is a measure of the degree of spike correlations that is preserved over different time scales. It falls between the topological dimension $D_T = 0$ and the Euclidian dimension $E = 1$ of a one-dimensional point process (or *dust*) (Mandelbrot, 1983). For the auditory neural spike train, the fractal dimension is appropriately defined as the exponent α in the Fano-factor time relation $F(T) \propto T^{\alpha}$ in the domain where it follows this power-law behavior. If the Fano factor is measured at two *sufficiently large* counting times, T_1 and T_2, then α may be estimated from the relation $F(T) \propto T^{\alpha}$ as:

$$\alpha \approx \frac{\log[F(T_2)/F(T_1)]}{\log (T_2/T_1)}. \tag{3}$$

Using this formula to calculate α for primary auditory neurons leads to values lying between 0.3 and 1.0. (For the data illustrated in Fig. 3, $\alpha \approx 0.68$.) It is important to note that a spike train of sufficiently long duration, typically several hundred seconds, is useful for obtaining a reliable estimate for α; the estimated value of α usually increases, and the variance of the estimate apparently decreases, with increasing L (Woo, 1991, Table 3.6). Furthermore, the value of α generally depends on which portion of a data set is examined.

V. Alteration of the Firing Pattern Engendered by Stimulation

The FFC (variance-to-mean ratio versus counting time T) for this same auditory neuron (unit A) is shown in Fig. 4 for driven activity collected for $L = 800$ s when the stimulus is a continuous tone at the CF (solid curve). The spontaneous data shown in Fig. 3 are repeated for comparison (dashed curve). Although the

FIGURE 3. Fano-factor time curve (FFC) for the spontaneous firing (no stimulus) of a primary auditory neuron (unit A) in an experiment of duration $L = 400$ s (dashed curve). The spontaneous rate fluctuations for this neuron are displayed in Fig. 1a. The Fano-factor time curve assumes a value of unity at short counting times, dips below unity for counting times $\gtrsim 1$ ms, and finally increases in pure power-law fashion when the counting time exceeds about 400 ms. In contrast, the FFC for a simulated dead-time-modified Poisson process (solid curve) remains approximately constant at a value below unity for all values of T larger than the dead time. The Fano factor for a Poisson point process in the absence of dead time is always precisely unity, whatever the value of T. From Teich *et al.* (1990b).

M. C. Teich, "Fractal Neuronal Firing Patterns," in Single Neuron Computation, edited by T. McKenna, J. Davis, and S. F. Zornetzer (Academic Press, Boston, 1992), ch. 22, pp. 589-625

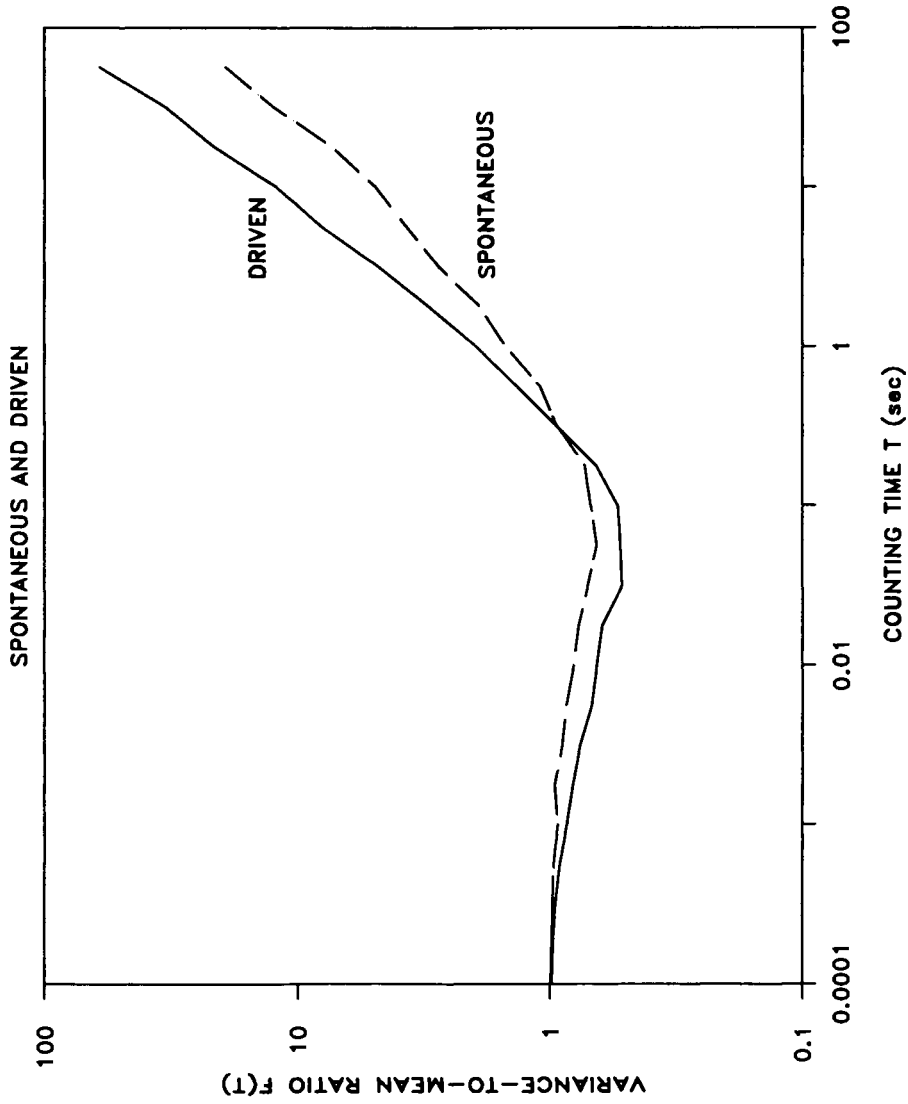

M. C. Teich, "Fractal Neuronal Firing Patterns," in Single Neuron Computation, edited by T. McKenna, J. Davis, and S. F. Zornetzer (Academic Press, Boston, 1992), ch. 22, pp. 589-625

shapes of the FFCs are similar, the minimum Fano factor F_{min} is lower under stimulation (because dead time has a greater effect on F when the rate is higher), and the power-law exponent is greater. (For this particular neuron, it increases from 0.68 to 0.85 when the tone is applied.) This represents an increase in the fractal dimension, indicating that an acoustic stimulus serves not only to alter the rate of action-potential firing but the pattern of firing as well. The presence of the stimulus results in larger rate fluctuations.

For driven firing, F typically assumes a minimum value F_{min} between about 0.5 and 0.9 at counting times in the tens of ms. The onset of pure power-law behavior (with exponents in the range between about 0.7 and 1.0) occurs at counting times between about 0.1 and 0.5 s. Figure 5 illustrates the change in the power-law exponent for several primary auditory neurons when continuous-tone stimulation is applied. For primary auditory neurons, this exponent, representing the fractal dimension, generally increases in the presence of such stimulation.

Because the power-law exponent associated with driven activity is generally greater than that associated with spontaneous activity, as shown in Fig. 5, estimates of the mean firing rate for driven activity will converge more slowly than estimates for spontaneous activity for integration times longer than several hundred milliseconds.

VI. Comparison of Auditory and Vestibular Firing Patterns

As a counterpoint to the behavior of primary auditory neurons, which have Fano factors substantially larger than zero even when the counting time is relatively short, spontaneously firing low-skew vestibular neurons have narrow PNDs and very small Fano factors. It is well-known that such neurons fire in a far more regular pattern than do auditory neurons (Walsh *et al.*, 1972). Indeed, the firing pattern of a low-skew vestibular neuron is similar to that of a mammalian retinal ganglion cell at high luminance levels (Barlow and Levick, 1969). In Figs. 6a and 6b, we present short-counting-time (T = 51.2 ms, 2,000 samples) and

FIGURE 4. Fano-factor time curve for continuous-tone-driven firing of unit A in an experiment of duration L = 800 s (solid curve). The Fano-factor time curve for the spontaneous firing of this neuron, shown in Fig. 3, is repeated here for purposes of comparison (dashed curve). The driven rate fluctuations for this cell are displayed in Fig. 2a. The shapes of the Fano-factor time curves are similar for the spontaneous and driven firing; however, the power-law exponent increases from 0.68 for spontaneous firing to 0.85 for driven firing. From Teich *et al.* (1990b).

M. C. Teich, "Fractal Neuronal Firing Patterns," in Single Neuron Computation, edited by T. McKenna, J. Davis, and S. F. Zornetzer (Academic Press, Boston, 1992), ch. 22, pp. 589-625

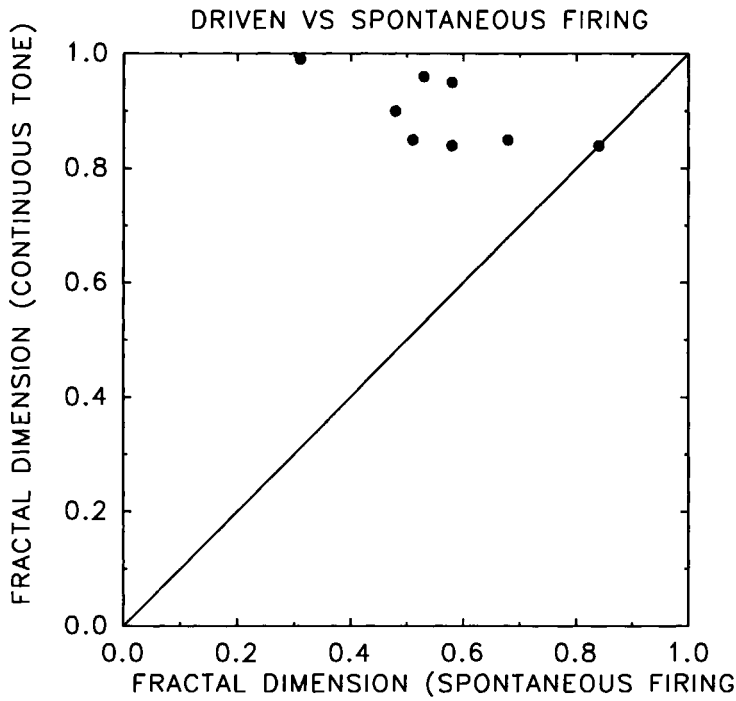

FIGURE 5. Relationship of the power-law exponents for several auditory neurons, under conditions of continuous-tone-driven and spontaneous firing. The exponent, which represents the fractal dimension of the process, generally increases under continuous-tone stimulation.

slightly longer counting-time (T = 204.8 ms, 500 samples) spontaneous vestibular PNDs (denoted VES), respectively, for one such low-skew cell. Both of these PNDs were constructed from the same neural spike train. They exhibit count means of 1.95 and 7.81, and Fano factors that are very low, $F(T = 51.2$ ms) = 0.04 and $F(T = 204.8$ ms) = 0.03, respectively. The small values of $F(T)$ indicate that these vestibular firings tick along with the near regularity of a clock, at least for counting times $\leq$204.8 ms. It will be of interest to measure vestibular PNDs using longer counting times.

The vestibular PNDs are compared with PNDs from auditory neurons (AUD), and from simulated-Poisson data (POI), all with the same approximate spike rate ($\approx$40 s^{-1}) for both counting times. Like the vestibular PNDs, the auditory PNDs were constructed from the same underlying sequence of neural events. It is clear from Fig. 6 that the vestibular PNDs are the narrowest of the three. For these particular counting times, the auditory PNDs are narrower than the simulated-Poisson PNDs, but for longer counting times this reverses. The scalloping

M. C. Teich, "Fractal Neuronal Firing Patterns," in Single Neuron Computation, edited by T. McKenna, J. Davis, and S. F. Zornetzer (Academic Press, Boston, 1992), ch. 22, pp. 589-625

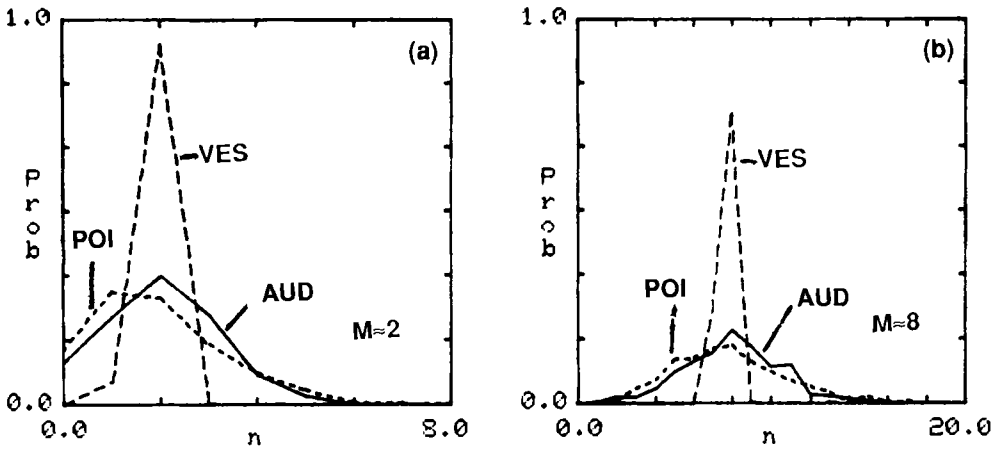

FIGURE 6. PNDs for cat vestibular (VES) and auditory (AUD) primary neurons, and simulated-Poisson (POI) data, with the same approximate spike rate ($\approx$ 40 s^{-1}). T = 51.2-ms PNDs are shown in a; T = 204.8-ms PNDs are shown in b. The vestibular PNDs have count means of 1.95 and 7.81, and Fano factors of 0.04 and 0.03 in a and b, respectively. The auditory data are drawn from Teich and Khanna (1985, Fig. 8) with stimulation at a frequency of 1,445 Hz and a level of 6 dB SPL. The auditory PNDs have count means of 2.01 and 8.03, and Fano factors of 0.70 and 0.81 in a and b, respectively. This particular data set was chosen because its spike rate is quite close to that of the vestibular neuron. The simulated-Poisson PNDs have count means of 1.92 and 7.85, and Fano factors of 1.02 and 1.08 in a and b, respectively. The number of samples is 2,000 and 500 for the short and longer counting-time vestibular PNDs, respectively, whereas it is 1,000 and 250 for the short and longer counting-time auditory and simulated-Poisson PNDs, respectively. From Teich (1989), © IEEE.

evident in the auditory PNDs (Teich and Turcott, 1988; Teich, 1989) appears to diminish as the number of samples increases.

VII. Fractal Firing Patterns at Higher Auditory Centers

Recent experiments carried out by Shofner and Dye (1989) in the gerbil (using a counting time of T = 400 ms) reveal similar behavior in the spike train at the cochlear nucleus, which derives its information from primary auditory nerve-fiber inputs.

We have carried out a preliminary analysis of single-neuron firing at the LSO, and fractal firing patterns may also be present at that locus (Turcott *et al.*, 1991). Because LSO neurons exhibit markedly nonstationary firing rates (in many cells

M. C. Teich, "Fractal Neuronal Firing Patterns," in Single Neuron Computation, edited by T. McKenna, J. Davis, and S. F. Zornetzer (Academic Press, Boston, 1992), ch. 22, pp. 589-625

the rate falls in approximately exponential fashion), we have had to remove the nonstationarity to expose the stochastic nature of the underlying point process.

Thus, the sequence of action potentials at three distinct loci in the mammalian auditory pathway (AN, CN, and LSO) all appear to share a similarity in the underlying stochastic point process: fractal neuronal firing patterns when the observation time is sufficiently large.

VIII. Neural Information Processing with Fractal Events

Why would auditory neuronal firing patterns exhibit fractal behavior and vestibular patterns not? Since the auditory neural-spike train appears to sample an information-carrying signal (Khanna and Teich, 1989a,b), we suggest that these unusual patterns may serve to sample fractal signals and natural fractal noises in an efficient correlated manner (Teich, 1989), Indeed, the instantaneous audio power of music and speech, and the instantaneous frequency (rate of zero crossings) of music, exhibit fractal ($1/f$-type) properties over a substantial range of low frequencies (Voss and Clarke, 1978). The potential benefits to be gained from such sampling, such as bandwidth compression, need to be established from an information-theoretic point of view.

An analogous argument for the visual system would suggest that fractal firing patterns may be present at loci where fractal image information is sampled, e.g., at the striate cortex. Indeed, spike bursts and recurrences of bursts do appear to occur at that locus (Legéndy and Salcman, 1985).

The vestibular system is designed to estimate angular acceleration with high accuracy. The information is slowly varying so that fractal behavior, if present, would be evident only for extremely long counting times. It will be of use to discover where fractal neuronal firing patterns do, and do not, occur as a prelude to understanding why they occur.

If fractal firings are useful for the sampling and decoding of fractal information-bearing signals, they are, by virtue of their noisiness, a liability for the detection of weak acoustic signals. Psychophysical tasks involving the detection of weak signals, such as intensity discrimination and loudness estimation, can be understood in terms of the relationship of the count variance to the count mean of an underlying point process representing neural activity (McGill and Teich, 1991a,b). Since the Fano-factor time curve for primary auditory fibers typically achieves its minimum value for counting times in the range of 50 to 500 ms, it would appear that the neural count at the periphery of the auditory system is least noisy over this range of integration times. Information processing tasks that rely on low variance for good performance would, it seems, be best served by using

M. C. Teich, "Fractal Neuronal Firing Patterns," in Single Neuron Computation, edited by T. McKenna, J. Davis, and S. F. Zornetzer (Academic Press, Boston, 1992), ch. 22, pp. 589-625

integration times in this range, and these psychophysical tasks do, indeed, exhibit behavior that appears to accord with this. Perhaps the system has its cake—and eats it, too—by making use of short integration times (to maximize signal-to-noise ratio) for tasks involving the detection, discrimination, and estimation of weak signals, and long integration times (to maximize memory) for tasks involving the extraction of information from strong fractal signals.

IX. Biophysical Origins of the Fractal Behavior

The mathematical point process used to describe the sequence of action potentials in the peripheral auditory system should be consistent with the underlying physiological behavior of the system. There are a number of possible origins of the observed fractal behavior, three of which appear to merit further consideration (Teich *et al.*, 1991):

1. Slow decay of intracellular calcium in the receptor hair cell.
2. Fractal ion-channel statistics (Liebovitch and Tóth, 1990; Teich, 1989).
3. Self-organized criticality in ion-channel behavior.

The first two of these models may be cast in the form of a *sick-time-modified* FDSPP.

X. Identifying the Mathematical Point Process

Three mathematical models are provided for describing the point process underlying auditory neural firings. The first model is applicable for an arbitrary stationary point process with constant rate; it therefore admits both correlation and dead (or sick) time. However, its range of prediction is limited to second-order statistics, e.g., quantities such as the FFC; it cannot be used to calculate measures such as the PND or PID. The second model is a *fractal doubly stochastic Poisson point process* (FDSPP) that we developed on the basis of plausible physiological arguments (Teich *et al.*, 1990a). The use of a specific model such as this has the advantage that its range of prediction is unlimited; any measure obtained from the neural events can, in principle, be calculated for the process. Although the inclusion of dead (or sick) time destroys the DSPP character of this process, thereby making it difficult to obtain analytical results, we have managed to incorporate the effects of refractoriness in a simulated version of the FDSPP. This process appears to behave very much like the neural events.

M. C. Teich, "Fractal Neuronal Firing Patterns," in Single Neuron Computation, edited by T. McKenna, J. Davis, and S. F. Zornetzer (Academic Press, Boston, 1992), ch. 22, pp. 589-625

The third model is a generalization of the first that is suitable for a time-varying rate or stimulus.

A. *General Stationary Point Process with Constant Rate*

For an arbitrary stationary point process with constant rate, there is a unique relation between the Fano-factor time curve $F(T)$ and the joint probability of event-pair coincidences $\lambda^2 g(\tau)$ (Cox and Lewis, 1966, pp. 72–75; Teich, 1989; Teich and Saleh, 1988, Eq. (2.16)):

$$F(T) = 1 + 2\lambda \int_0^T \left(1 - \frac{\tau}{T}\right) [g(\tau) - 1]\, d\tau. \tag{4}$$

Here, λ is the mean rate of the point process, and τ is the delay time between the events. The normalized coincidence rate $g(\tau)$ plays the role of the correlation function for continuous processes.

A simple coincidence rate may be constructed by including idealized models of absolute refractoriness and correlation:

(1) For delay times less than the average refractory period τ_d, the coincidence rate is taken to be zero, since action potentials cannot follow one another within this time.
(2) At the termination of the refractoriness period, the normalized coincidence rate rises abruptly to unity, since the event occurrences are then presumed to be uncorrelated.
(3) Finally, for delay times longer than the fractal onset time τ_f, the normalized coincidence rate increases above unity and falls in power-law fashion toward unity, representing a slowly decreasing correlation of the spike occurrences with increasing delay time.

The idealized normalized coincidence rate is then:

$$g(\tau) = \begin{cases} 0, & |\tau| < \tau_d, \\ 1, & \tau_d \leq |\tau| \leq \tau_f, \\ 1 + \dfrac{\delta}{\lambda}\left(\dfrac{|\tau|}{\tau_f}\right)^{\alpha - 1}, & |\tau| > \tau_f, \end{cases} \tag{5}$$

where δ is a constant (units of s^{-1}), and $\alpha - 1$ $(0 < \alpha < 1)$ is the power-law exponent of the normalized delay time. The correlation between a pair of spikes is typically rather small; values of δ/λ typically range from 0.02 to 0.04, and

M. C. Teich, "Fractal Neuronal Firing Patterns," in Single Neuron Computation, edited by T. McKenna, J. Davis, and S. F. Zornetzer (Academic Press, Boston, 1992), ch. 22, pp. 589-625

seldom stretch above 0.1. Equation (5) is a generalized form of Eq. (4) in Teich (1989); the power-law exponent is $\alpha - 1$ rather than $-\frac{1}{2}$, and δ/λ is used in place of δ. A more realistic coincidence rate would rise gradually, rather than abruptly, to account for relative refractoriness (Teich, 1989).

Substituting this coincidence rate into Eq. (4) leads to a Fano-factor time function given by:

$$F(T) = \begin{cases} 1 - \lambda T, & T < \tau_d \\ 1 - \lambda\tau_d[2 - \tau_d/T], & \tau_d \leq T \leq \tau_f \\ 1 - \lambda\tau_d[2 - \tau_d/T] + \dfrac{2}{\alpha(\alpha + 1)}\,\delta\tau_f[(T/\tau_f)^\alpha + \alpha(\tau_f/T) - (\alpha + 1)], & T > \tau_f. \end{cases} \tag{6}$$

Equation (6) is a generalization of Eq. (5) in Teich (1989); the power-law exponent is α rather than $\frac{1}{2}$, and the power-law term has a coefficient proportional to $\delta\tau_f$ rather than $\delta\lambda\tau_f$. (This accommodates the empirical independence of δ, as defined in Eq. (6), on λ, and results from the use of the coefficient δ/λ in Eq. (5).) Each of the five panels in Fig. 7 illustrates the dependence of $F(T)$, as given in Eq. (6), on one of the essential parameters: λ, τ_d, δ, τ_f, and α. For purposes of illustration, we use parameters with physiologically reasonable values, *viz.*, $\lambda = 100\ s^{-1}$, $\tau_d = 1.5$ ms, $\delta = 2\ s^{-1}$, $\tau_f = 0.1$ s, and $\alpha = 0.5$. As expected, the theoretical curves always assume a value of unity as $T \to 0$, and dip below unity as T increases and dead time comes into play. The power-law growth of the Fano factor for large T, $F(T) \propto (T/\tau_f)^\alpha$, follows from the delay-time dependence of the coincidence rate for large τ, $g(\tau) - 1 \propto (|\tau|/\tau_f)^{\alpha-1}$. Although the correlation between a single pair of spikes is typically rather small, the Fano factor can become quite large since it integrates the many correlations from different pairs of spikes within the time window T. (See Eq. (4).)

We have used Eq. (6) (with the value of λ set at the experimental spike rate), in conjunction with the curve-fitting routine in Jandel Scientific's Sigma-Plot™ software package (version 4.0), to fit the FFCs of eight primary auditory nerve-fiber spike trains, both in the presence and in the absence of a pure-tone stimulus. The software routine makes use of the Marquardt–Levenberg algorithm, which finds parameters that minimize the square difference of the theory and data. We chose to minimize the square difference of the logarithms of the theory and data. The results shown in Fig. 8 for unit A are typical; the theoretical variance-to-mean ratio $F(T)$ given in Eq. (6) nicely describes both the spontaneous and

M. C. Teich, "Fractal Neuronal Firing Patterns," in Single Neuron Computation, edited by T. McKenna, J. Davis, and S. F. Zornetzer (Academic Press, Boston, 1992), ch. 22, pp. 589-625

driven experimental data (which is the same data as shown in Fig. 4) with reasonable physiological parameters. Evidently, the idealized coincidence rate postulated in Eq. (5) captures the essential elements inherent in auditory neuronal firing patterns (refractoriness and decaying power-law correlation with Poisson underlying events), at least to second order. The theory is, of course, least satisfactory in the region where relative refractoriness plays its principal role, *viz.*, from about 1 to 40 ms. The best-fitting parameters for all eight units, using Eq. (6), are compared under conditions of continuous-tone stimulation at the CF, and spontaneous firing, in Fig. 9. Aside from causing λ to increase, the presence of the tone generally causes α to increase; however, it appears to have little effect on τ_d, τ_f, and δ. The durations of these experiments range from 50 to nearly 2,000 s.

The power spectral density $S(f)$ of a random process, when it exists, is

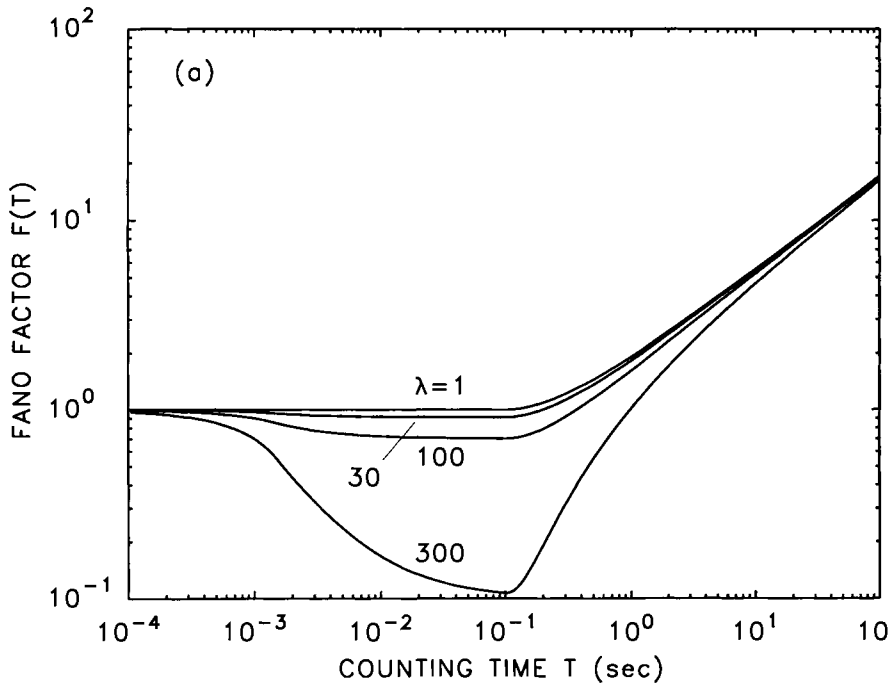

FIGURE 7. Variance-to-mean ratio $F(T)$ versus counting time T plotted in accordance with Eq. (6), using the default parameters $\lambda = 100\ s^{-1}$, $\tau_d = 1.5$ ms, $\delta = 2\ s^{-1}$, $\tau_f = 0.1$ s, and $\alpha = 0.5$. (a) Behavior of $F(T)$ for different values of λ. (b) Behavior of $F(T)$ for different values of τ_d. (c) Behavior of $F(T)$ for different values of δ. (d) Behavior of $F(T)$ for different values of τ_f. (e) Behavior of $F(T)$ for different values of α.

M. C. Teich, "Fractal Neuronal Firing Patterns," in Single Neuron Computation, edited by T. McKenna, J. Davis, and S. F. Zornetzer (Academic Press, Boston, 1992), ch. 22, pp. 589-625

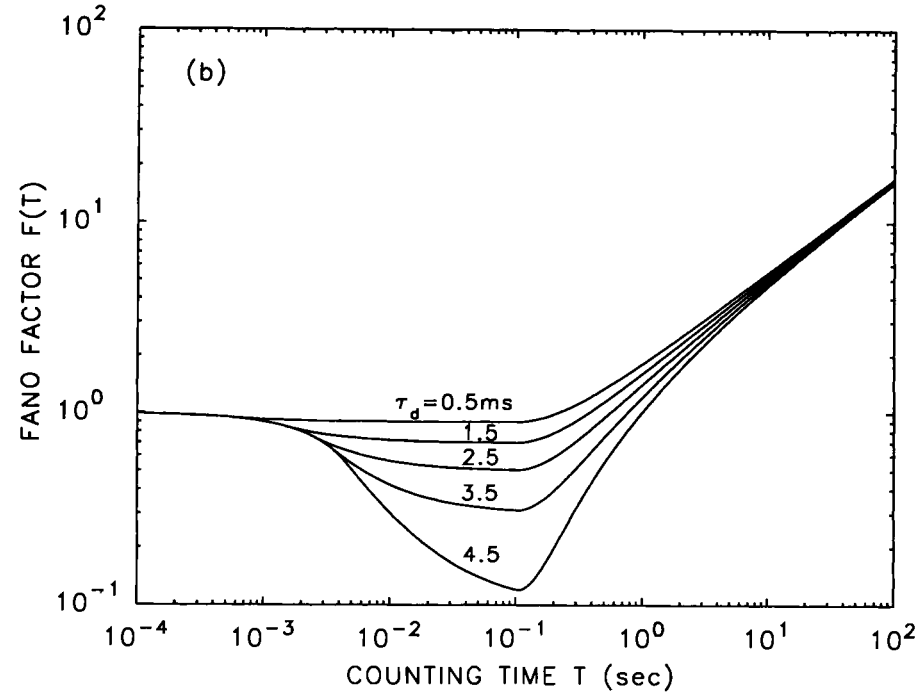

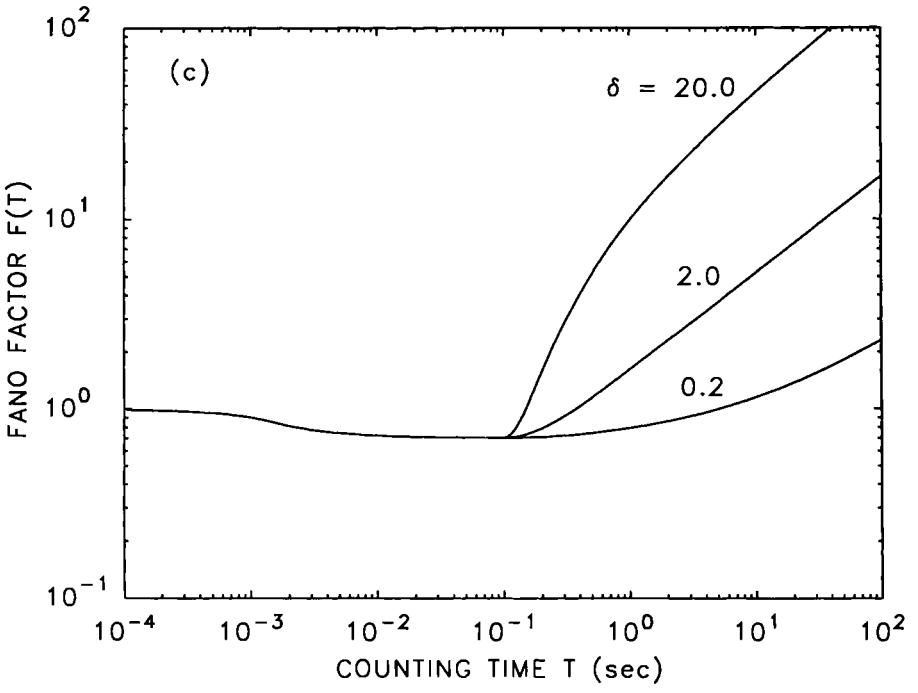

M. C. Teich, "Fractal Neuronal Firing Patterns," in Single Neuron Computation, edited by T. McKenna, J. Davis, and S. F. Zornetzer (Academic Press, Boston, 1992), ch. 22, pp. 589-625

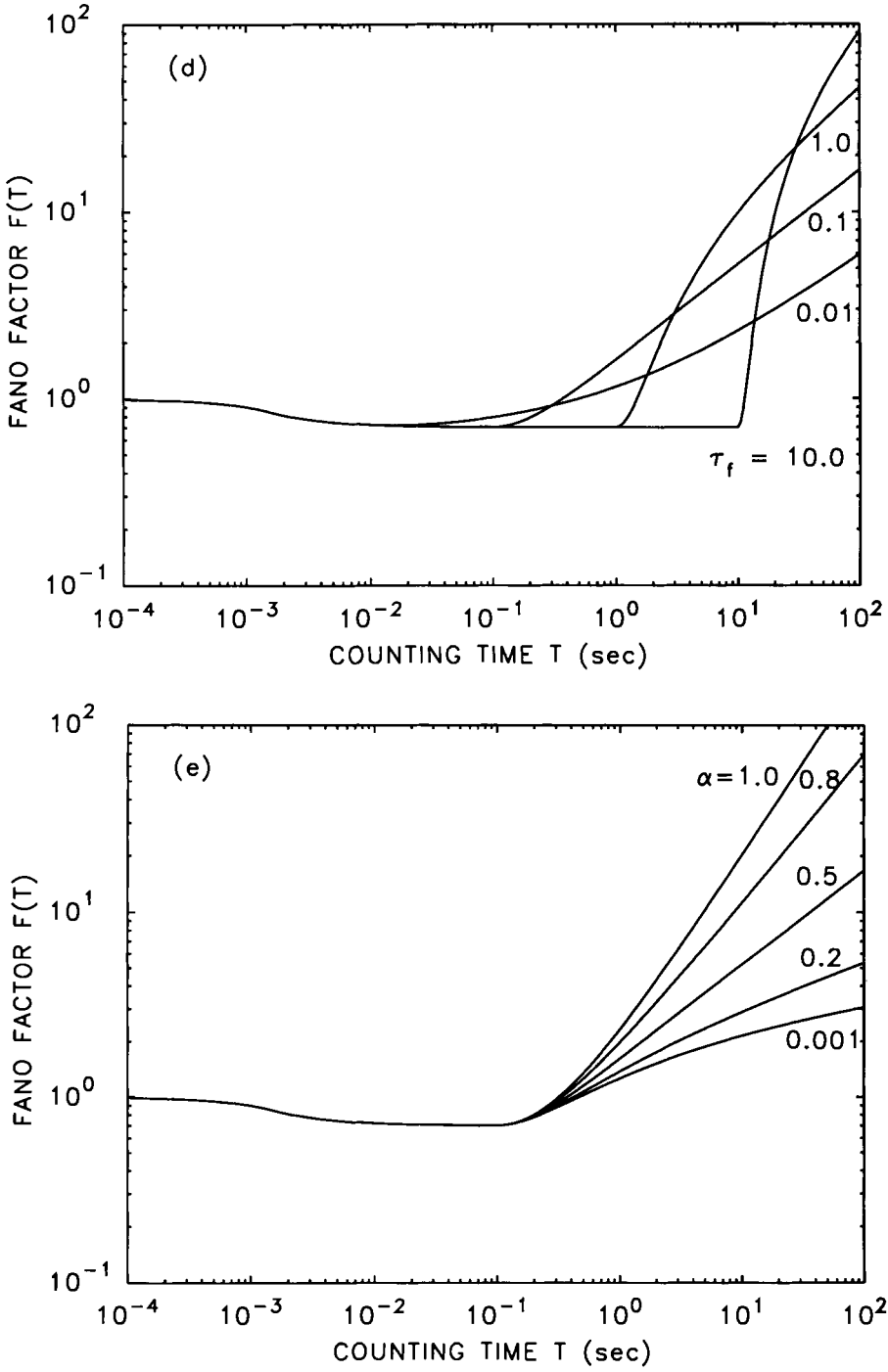

FIGURE 7. *Continued*

M. C. Teich, "Fractal Neuronal Firing Patterns," in Single Neuron Computation, edited by T. McKenna, J. Davis, and S. F. Zornetzer (Academic Press, Boston, 1992), ch. 22, pp. 589-625

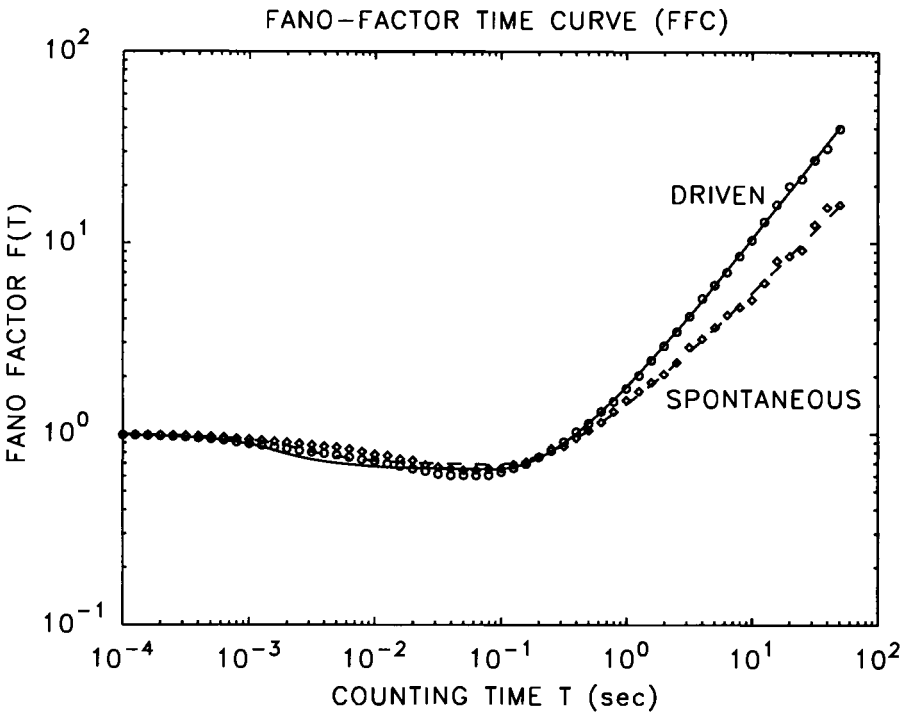

FIGURE 8. Fit of the theoretical Fano factor given in Eq. (6) (dashed and solid curves) to spontaneous and driven experimental data points for unit A. For the spontaneous fits, the parameters take on the physiologically plausible values $\lambda = 65\ s^{-1}$, $\tau_d = 2.4$ ms, $\delta = 1.34\ s^{-1}$, $\tau_f = 87$ ms, and $\alpha = 0.68$. For the driven fits, the parameter values are $\lambda = 113\ s^{-1}$, $\tau_d = 1.6$ ms, $\delta = 1.63\ s^{-1}$, $\tau_f = 88$ ms, and $\alpha = 0.85$.

determined from the coincidence rate by means of the Wiener–Khinchin theorem. When $g(\tau)$ takes the form indicated in Eq. (5), $S(f)$ behaves as

$$S(f) \propto (1/\lambda) f^{-\alpha}, \quad f \leq f_f, \tag{7}$$

in the low-frequency (large delay-time) regime. The quantity f_f is the fractal cutoff frequency; it is inversely proportional to τ_f. Since $0 < \alpha < 1$, this represents $1/f$-type noise (Woo *et al.*, 1992).

With this model in hand, we may now quantitatively consider the self-similarity of the rate fluctuations illustrated in Figs. 1a and 2a. Our considerations are restricted to counting times sufficiently long so that we are in the power-law (fractal) regime. The degree to which a process with firing rate λ_T may be considered to be self-similar is established by determining the dependence of its standard deviation σ_λ on the time window T. Since $\lambda_T = n/T$, where n is the random number of neural spikes in the time T, the variance of the firing rate is

M. C. Teich, "Fractal Neuronal Firing Patterns," in Single Neuron Computation, edited by T. McKenna, J. Davis, and S. F. Zornetzer (Academic Press, Boston, 1992), ch. 22, pp. 589-625

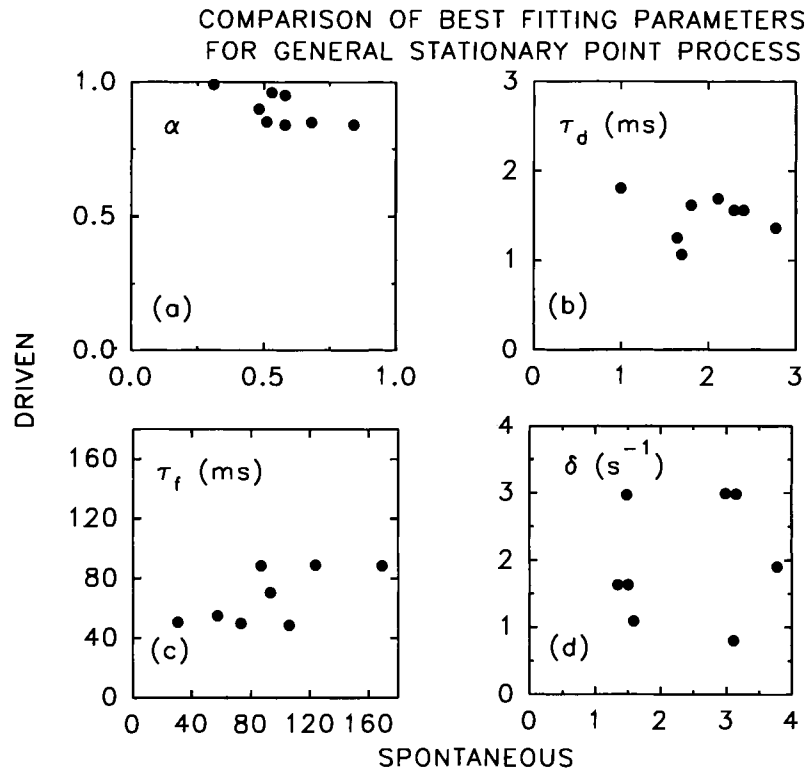

FIGURE 9. Comparison of best-fitting parameters for eight units, under driven and spontaneously active firing conditions, using Eq. (6) for the variance-to-mean ratio.

$\mathrm{Var}(\lambda_T) = (1/T^2)\mathrm{Var}(n)$. By definition, however, $\mathrm{Var}(n) = \langle n \rangle F(T)$, where $\langle n \rangle$ is the mean number of events in the time T, and F is the Fano factor, so that $\mathrm{Var}(\lambda_T) = (1/T^2)\langle n \rangle F(T)$. Since $\langle n \rangle \propto T$ and $F(T) \propto T^{\alpha}$ for sufficiently large T, we obtain:

$$\mathrm{Var}(\lambda_T) \propto \frac{1}{T^{1-\alpha}}. \tag{8}$$

The standard deviation of the rate therefore is given by

$$\sigma_\lambda \propto \frac{1}{T^{(1-\alpha)/2}}. \tag{9}$$

Non-fractal processes have a fractal dimension $\alpha = 0$, so that the standard deviation of the rate is proportional to $1/T^{1/2}$; thus, the rate converges relatively quickly with increased averaging. Processes with $\alpha \rightarrow 1$ have a standard deviation

M. C. Teich, "Fractal Neuronal Firing Patterns," in Single Neuron Computation, edited by T. McKenna, J. Davis, and S. F. Zornetzer (Academic Press, Boston, 1992), ch. 22, pp. 589-625

that is independent of T so that there is no convergence with time averaging, and the rate process is fully self-similar. Estimates of the mean rate, therefore, converge more slowly with increasing T for fractal processes than for non-fractal processes, with the rate of convergence depending on the fractal dimension α. In the region where refractoriness is operative (below several hundred milliseconds), the process is non-fractal and the standard deviation of the rate behaves as $1/T^{1/2}$. The firing rate, therefore, is most accurately estimated by using counting times in this range.

B. Fractal Doubly Stochastic Poisson Point Process

The approach presented in the preceding, though valid for an arbitrary stationary point process, is based on a phenomenological construct for the coincidence rate and is limited to providing second-order, and some first-order, statistics. We have developed a particular type of fractal point process, the *dead-time-modified fractal doubly stochastic Poisson point process* (FDSPP), that exhibits behavior consistent with all of the experimental statistics of spontaneous and pure-tone-driven VIIIth-nerve action potentials examined to date, including the pulse-number and interspike-interval distributions.

Particular attention is devoted to two specific examples of this process: the *fractal-shot-noise-driven* (FSND) DSPP and one of its special cases, the *fractal-Gaussian-noise-driven* (FGND) DSPP (Lowen and Teich, 1991). Fractal behavior in the FSND DSPP is assured by choosing an impulse-response function that decays in a power-law manner with a certain range of exponents. This particular process is physiologically plausible for certain nerve-spike generation models, as mentioned in Section IX. Analytical results have been derived for many features of this process, including the coincidence rate, Fano factor, and spectrum. For the range of parameters of interest to the problem at hand, and for sufficiently long delay and counting times, these latter quantities turn out to be [Lowen and Teich, 1991, Eqs. (37), (48), and (52)]:

$$g(\tau) = 1 + (k_1/\lambda)|\tau|^{\alpha-1}, \tag{10}$$

$$F(T) = 1 + k_2 T^{\alpha}, \tag{11}$$

and

$$S(f) = (k_3/\lambda) f^{-\alpha}, \tag{12}$$

where k_1, k_2, and k_3 are constants. These equations assume the same form as those set forth in Eqs. (5)–(7) in Section X.A. This is expected, since we are limiting our attention to long delay and counting times where the effects of dead

M. C. Teich, "Fractal Neuronal Firing Patterns," in Single Neuron Computation, edited by T. McKenna, J. Davis, and S. F. Zornetzer (Academic Press, Boston, 1992), ch. 22, pp. 589-625

time are negligible, and both approaches incorporate a power-law decreasing coincidence rate. Since the phenomenological Fano factor developed in Section X.A is in accord with the FFC data, obviously Eq. (11) will be too.

In the case of the FDSPP, however, we have knowledge of the full point process. This allows us to calculate other measures (e.g., the PND and PID, as well as the serial count correlation coefficient (SCC) and rescaled range analysis (R/S), both of which will be explained shortly), and to compare them with the neural data. We can, therefore, perform more stringent tests for identifying the mathematical point process that characterizes auditory neuronal firings.

Indeed, the collection of data in the form of the PID, PND, FFC, SCC, and R/S provides a rather comprehensive picture of a neural spike train and enables us to make reasonable conjectures about the underlying mathematical point process (Teich *et al.*, 1990a). The PID, PND, and FFC are, by now, well-known statistics that have been described in detail elsewhere (Teich, 1989; Teich and Khanna, 1985; Teich and Turcott, 1988).

The SCC and R/S provide estimates of the degree of serial correlation in the data set. The SCC gives the correlation between the numbers of neural spikes in adjacent counting periods, and is generally a function of the counting time

---

FIGURE 10. (a) Pulse-number distribution (PND) constructed from the spontaneous spike train of auditory unit A (as in Figs. 1a, 3, and 8), using a counting time $T = 1$ sec (solid curve). PNDs obtained from simulations of three theoretical models are also shown. The model parameters were chosen to give the same mean count as the data. The PND obtained from the FDSPP resembles the data. On the other hand, the PND obtained from the dead-time-modified Poisson point process (DTMP, denoted PP here) is narrower than the data, while that obtained from the renewal fractal process (RFP) is far broader than the data. (b) The Fano-factor time curve (FFC) is constructed from the PND. For auditory-nerve data, $F(T)$ typically grows in power-law fashion as T^{α} $(0 < \alpha < 1)$ for sufficiently large counting times T, implying a power-law-decreasing normalized coincidence rate and a power-law form for the power spectral density at low frequencies. Again the FFC obtained from the FDSPP resembles the data quite closely, whereas the FFCs of the PP and the RFP deviate substantially from it, even though the latter does exhibit power-law behavior. (c) For the PP, $\alpha = 0$, so that $C(T) = 0$ for the serial count correlation coefficient (SCC), as is evident in the figure for sufficiently large counting times. (The dip in the curve in the vicinity of 2 msec, which arises from dead time, would be moderated were sick time used instead.) Once again the SSC obtained from the FDSPP closely resembles the data, while the SSCs associated with the PP and the RFP deviate substantially from it. (d) In rescaled range (R/S) analysis, the renewal nature of the PP and RFP cause $R(k)$ to behave as $k^{\frac{1}{2}}$, where k is the number of interspike intervals; the data and the results from the FDSPP rise more steeply, indicating positive correlation for collections of large numbers of interspike intervals. From Teich *et al.* (1990a).

M. C. Teich, "Fractal Neuronal Firing Patterns," in Single Neuron Computation, edited by T. McKenna, J. Davis, and S. F. Zornetzer (Academic Press, Boston, 1992), ch. 22, pp. 589-625

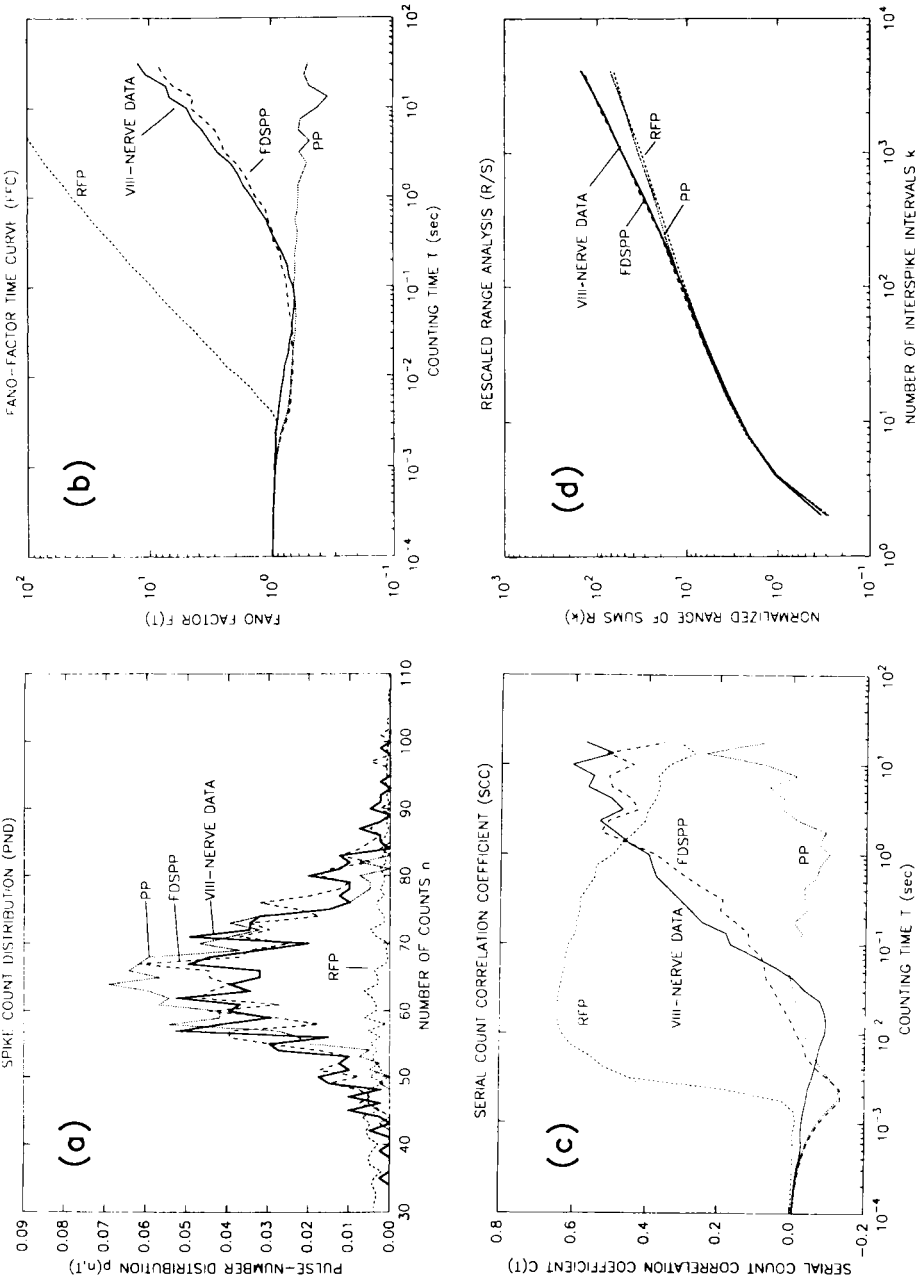

M. C. Teich, "Fractal Neuronal Firing Patterns," in Single Neuron Computation, edited by T. McKenna, J. Davis, and S. F. Zornetzer (Academic Press, Boston, 1992), ch. 22, pp. 589-625

T. In the domain of counting times where the Fano-factor time curve behaves as T^{α}, the serial count correlation coefficient $C(T)$ plateaus at the value $2^{\alpha} - 1$, as required by the relation between these measures.

Whereas the SCC reflects correlations between successive counts, the R/S parameter reflects correlations among interspike intervals. This measure is obtained by first estimating the interval mean and standard deviation in a block of interspike intervals of size k. For each of the k intervals, the difference between the value of the interval and the mean value is obtained and the result is successively added to a cumulative sum. The range is defined as the difference between the maximum and minimum values achieved within the cumulative sum, and this is normalized by the sample standard deviation to give $R(k)$. The normalized range of sums $R(k)$ is estimated for increasing values of k and plotted against k. With $R(k)$ proportional to k^h, $h > 0.5$ indicates positive correlation, $h < 0.5$ indicates negative correlation, and $h = 0.5$ indicates uncorrelated intervals (Hurst, 1951; Feller, 1951). This measure has the advantage of being valid even when the data exhibit extremely long-term correlations, as well as large (or infinite) variance; these are characteristics that can cause a process to appear nonstationary and, consequently, seriously impair the usefulness of standard measures (Mandelbrot, 1983).

We have compared the experimental behavior of these various statistics with those predicted by several theoretical models, including the dead-time-modified Poisson point process (DTMP), the dead-time-modified renewal fractal point process (RFP), as described by Teich *et al.* (1990a), and the dead-time-modified FDSPP described here. We have performed simulations using various forms of this latter process, and found that both the FSND DSPP and the FGND DSPP exhibit behavior that accords with all of these statistics. The DTMP and RFP, in contrast, do not.

The FDSPP—and, in particular, the FSND DSPP and the FGND DSPP—give results that are largely indistinguishable from the experimental statistics both for spontaneous firings (Fig. 10) and driven firings (Fig. 11), and we have identified

FIGURE 11. (a) PND (T = 1 sec), (b) FFC, (c) SCC, and (d) R/S constructed from the same 800-s driven spike train of unit A as that used in Figs. 2a, 4, and 8. The renewal processes are not represented, since their behavior is similar to that indicated in Fig. 10. The fractal dimension revealed by the slope of the FFC curve is greater than the value observed in Fig. 10b for spontaneous firing. The larger FFC exponent is reflected in a larger serial count correlation estimate, as is evident in the SCC curve. (Compare with Fig. 10c.) The increase in α and $C(T)$ under stimulation has been observed in all primary auditory-nerve cells examined to date. From Teich *et al.* (1990a).

M. C. Teich, "Fractal Neuronal Firing Patterns," in Single Neuron Computation, edited by T. McKenna, J. Davis, and S. F. Zornetzer (Academic Press, Boston, 1992), ch. 22, pp. 589-625

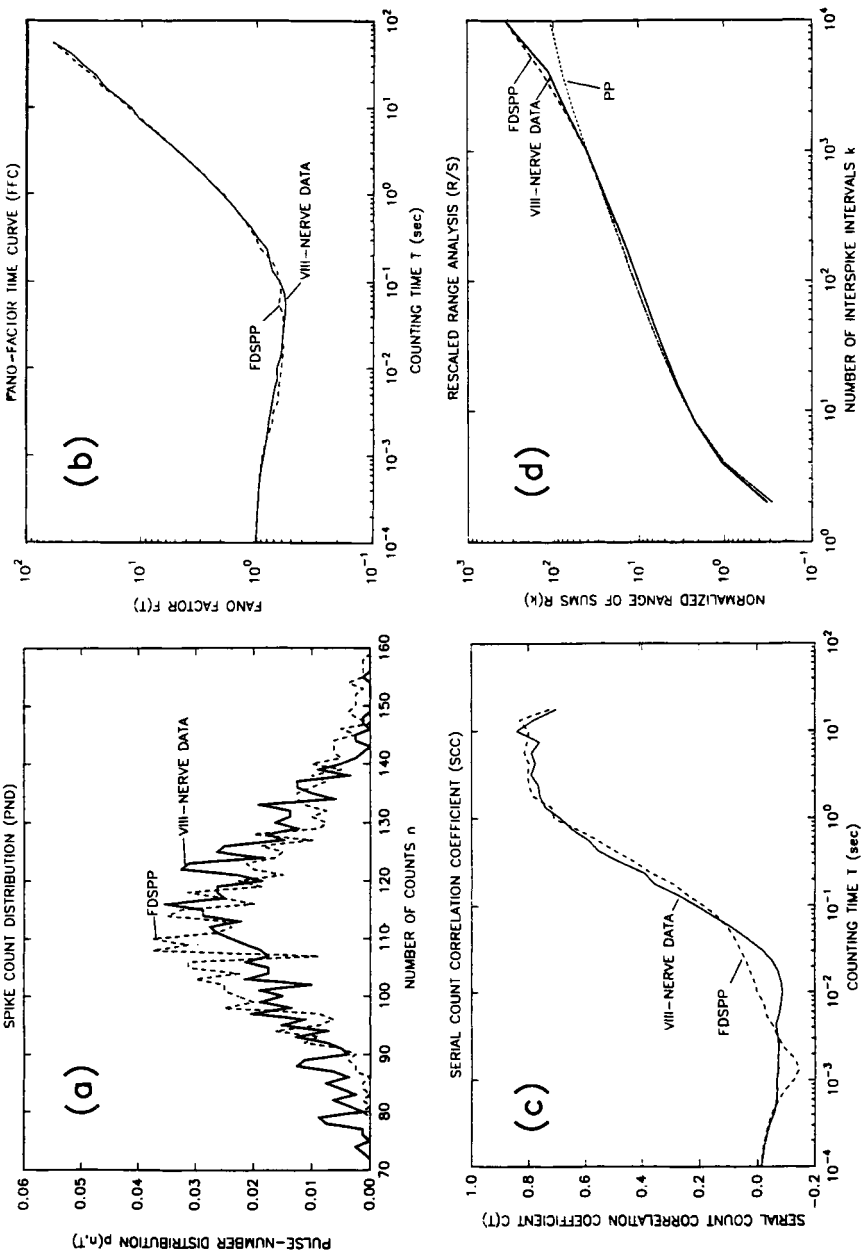

M. C. Teich, "Fractal Neuronal Firing Patterns," in Single Neuron Computation, edited by T. McKenna, J. Davis, and S. F. Zornetzer (Academic Press, Boston, 1992), ch. 22, pp. 589-625

the FDSPP as the point process that characterizes the auditory neural spike train (Teich *et al.*, 1990a). The essence of its behavior arises from Poisson underlying events with decaying power-law correlations.

These correlations can be removed by randomly shuffling the interspike intervals, for both spontaneous and driven data, as shown by Teich *et al.* (1990a). The shuffling serves to destroy the long-term correlations inherent in the ordering of the individual events. Indeed, shuffling alters the experimental measures, and their FDSPP theoretical counterparts, in precisely the same way.

C. *General Point Process with Variable Rate*

The formulas provided in Sections X.A and X.B are not applicable when the mean rate is varying (either deterministically or stochastically). This is the case, for example, when the stimulus is Gaussian noise or an information-bearing signal that varies with time, rather than a pure tone, or when adaptation is present. The stimulus itself then introduces another degree of variability, and the results described previously must be generalized to account for this. The resulting process will be a *triply stochastic Poisson point process* (TSPP), with three forms of stochasticity arising from:

1. Rate variations associated with adaptation and/or stimulus variability.
2. A biophysical mechanism involving long-term correlations.
3. An action-potential generation mechanism involving intrinsic auditory-neuron fluctuations and refractoriness.

Consider an arbitrary counting distribution $p(n,T|W)$ conditioned on an integrated rate (energy) W given by:

$$W = \int_{t_0}^{t_0+T} \lambda_t \, dt, \tag{13}$$

where λ_t is the time-varying rate, t_0 is the beginning of the counting interval, and T is the counting time (Cox and Lewis, 1966; Prucnal and Teich, 1979). If the rate λ_t is constant (homogeneous) and fixed at λ_0, the integrated rate W is simply $\lambda_0 T$.

On the other hand, if the rate λ_t exhibits a stochastic or deterministic time dependence, with characteristic time τ_c, the integrated rate W may be described in terms of a probability density function $P(W)$. When $T \gg \tau_c$, depending on the nature of the fluctuations of λ_t, W may become constant, in which case the results become identical to those for a homogeneous rate; in the other limit, when $T \ll \tau_c$, λ_t may be considered to be slowly varying, so that it can be removed from the integral, whereupon

M. C. Teich, "Fractal Neuronal Firing Patterns," in Single Neuron Computation, edited by T. McKenna, J. Davis, and S. F. Zornetzer (Academic Press, Boston, 1992), ch. 22, pp. 589-625

$$W = \lambda_t T, \tag{14}$$

and the statistics of W mimic those of λ_t.

Removing the conditioning from $p(n,T|W)$ provides the unconditional counting distribution $p(n,T)$ and the PND statistics in the presence of the stimulus or rate fluctuations,

$$p(n,T) = \int_W p(n,T|W)\, P(W)\, dW. \tag{15}$$

Equation (15) reveals that the counting distribution of the underlying kernel obtained in the absence of rate variations is smeared (broadened) by these variations. Note that the kernel, although often taken to be Poisson (Cox and Lewis, 1966; Prucnal and Teich, 1979), can assume an arbitrary form, such as that associated with the DTMP distribution (Cantor and Teich, 1975), a fractal counting distribution, or the Neyman Type-A distribution (Teich, 1981).

Using Eq. (15) to calculate the unconditional mean of $p(n,T)$, we find

$$\begin{aligned}\langle n\rangle &= \sum_{n=0}^{\infty} np(n,T) = \int_W dW\, P(W) \left[\sum_{n=0}^{\infty} np(n,T|W)\right] \\ &= \int_W dW\, P(W)\, \langle n|W\rangle = \int_W dW\, P(W)\, W = \langle W\rangle,\end{aligned} \tag{16}$$

provided that

$$\langle n|W\rangle = W. \tag{17}$$

This indicates that the mean integrated rate $\langle W\rangle$ is sufficient for calculating the unconditional mean count $\langle n\rangle$.

The unconditional variance is also readily calculated for processes with known conditional variance. Again, using Eq. (15), the unconditional mean-square count is:

$$\langle n^2\rangle = \sum_{n=0}^{\infty} n^2 p(n,T) = \int_W dW\, P(W)\, \langle n^2|W\rangle. \tag{18}$$

The conditional mean-square count is, of course, expressible in terms of the conditional variance and conditional mean as:

$$\langle n^2|W\rangle = \mathrm{Var}(n|W) + \langle n|W\rangle^2. \tag{19}$$

For auditory neurons with a constant mean rate, the conditional variance is related to the conditional mean by the conditional Fano factor $F(T|W)$ given in Eq. (6):

$$\mathrm{Var}(n|W) = F(T|W)\langle n|W\rangle. \tag{20}$$

M. C. Teich, "Fractal Neuronal Firing Patterns," in Single Neuron Computation, edited by T. McKenna, J. Davis, and S. F. Zornetzer (Academic Press, Boston, 1992), ch. 22, pp. 589-625

Thus, since $\langle n|W\rangle = W$,

$$\langle n^2|W\rangle = F(T|W)\langle n|W\rangle + \langle n|W\rangle^2 = F(T|W)W + W^2. \tag{21}$$

Using Eq. (21) in Eq. (18) provides:

$$\langle n^2\rangle = \int_W dW\, P(W)\, [F(T|W)W + W^2]. \tag{22}$$

We can now make use of an abbreviated form of Eq. (6), valid when the dead time can be ignored,

$$F(T|W) \approx 1 + c_1, \tag{23}$$

where c_1 is a function of α, δ, τ_f, and T. To facilitate the analysis, c_1 is assumed to be independent of λ and therefore W, as is often the case. Inserting Eq. (23) into Eq. (22), we obtain:

$$\langle n^2\rangle = \langle W\rangle + c_1\langle W\rangle + \langle W^2\rangle, \tag{24}$$

so that

$$\mathrm{Var}(n) = \langle n^2\rangle - \langle n\rangle^2 = \langle W\rangle + c_1\langle W\rangle + (\langle W^2\rangle - \langle W\rangle^2). \tag{25}$$

Finally, then, the Fano factor in the presence of rate variations turns out to be:

$$F(T) = \frac{\mathrm{Var}(n)}{\langle n\rangle} = 1 + c_1 + F_W, \tag{26}$$

where

$$F_W = \frac{\mathrm{Var}(W)}{\langle W\rangle} = \frac{\langle W^2\rangle - \langle W\rangle^2}{\langle W\rangle}. \tag{27}$$

Equation (26) represents the Fano factor associated with a triply stochastic distribution: when the kernel is Poisson ($c_1 = 0$), we obtain the well-known doubly stochastic Poisson result, $F(T) = 1 + F_W$ (Teich and Saleh, 1988). When, in addition, the rate is nonvarying, $F_W = 0$ and we obtain the homogeneous Poisson result, $F(T) = 1$ for all T.

We may examine the dependence of the unconditional Fano factor in Eq. (26) on the counting time by explicitly writing c_1 in terms of its dependence on T:

$$F(T) \approx 1 + \frac{2}{\alpha(\alpha + 1)}\,\delta\tau_f\left(\frac{T}{\tau_f}\right)^{\alpha} + F_W. \tag{28}$$

For linearly and exponentially varying rates (Prucnal and Teich, 1979), and for the intensity fluctuations of Gaussian noise (Teich and Saleh, 1988, Eq. (2.19)),

M. C. Teich, "Fractal Neuronal Firing Patterns," in Single Neuron Computation, edited by T. McKenna, J. Davis, and S. F. Zornetzer (Academic Press, Boston, 1992), ch. 22, pp. 589-625

$F_W = \langle\lambda\rangle T/M$, where M is a degrees-of-freedom parameter that is an increasing function of T, so that Eq. (28) becomes:

$$F(T) \approx 1 + \frac{2}{\alpha(\alpha + 1)} \delta\tau_f \left(\frac{T}{\tau_f}\right)^{\alpha} + \frac{\langle\lambda\rangle T}{M}. \tag{29}$$

Finally, then, the dependence of the unconditional Fano factor on the mean rate $\langle\lambda\rangle$ and on the counting time T is contained in the succinct expression:

$$F(T) \approx 1 + c_2 T^{\alpha} + \frac{\langle\lambda\rangle T}{M}, \tag{30}$$

where $c_2 = 2\delta\tau_f^{1-\alpha}/\alpha(\alpha + 1)$.

We conclude that the dependence of the Fano-factor time curve on the counting time T comprises two components in the long-counting time limit: The first increases as T^{α}, as in the case of pure-tone stimulation; the second increases with T/M (where M itself depends on T) and arises from mean rate fluctuations. This result is based on certain specific characteristics for the rate fluctuations (e.g., exponential or linear variation, or integrated intensity fluctuations associated with Gaussian noise) and is predicated on the counting time being large. A more detailed analysis of this general case can be obtained on the basis of the moment-generating functional for cascades of filtered Poisson point processes (Matsuo *et al.*, 1982).

We now explicitly consider a nonstationary rate arising from adaptation rather than from a stochastic stimulus. In auditory theory, two useful examples emerge in this context (Harrison, 1985; Lütkenhöner and Smith, 1986). The first is provided by an instantaneous rate λ_t that linearly decreases from a maximum value λ_{max} to a minimum value λ_{min}. For a deterministic nonstationarity such as this, the duration of the experiment L plays the role of τ_c because the rate continues to change continuously over L. In auditory experiments, $T \ll L$ so that the linearly advancing starting time t_0 of successive counting intervals serves to uniformly and exhaustively sample the rate over its entire range. In this case, the probability density function $P(\lambda)$ is easily shown to be uniformly distributed on the interval $[\lambda_{min},\lambda_{max}]$, with mean (Prucnal and Teich, 1979; Teich and Diament, 1969)

$$\langle\lambda\rangle = \frac{\lambda_{max} + \lambda_{min}}{2} \tag{31}$$

and variance

$$\mathrm{Var}(\lambda) = \frac{(\lambda_{max} - \lambda_{min})^2}{12}. \tag{32}$$

M. C. Teich, "Fractal Neuronal Firing Patterns," in Single Neuron Computation, edited by T. McKenna, J. Davis, and S. F. Zornetzer (Academic Press, Boston, 1992), ch. 22, pp. 589-625

Alternatively, λ_{min} can be expressed in terms of λ_{max}, L, and the slope of the decline.

The second example is embodied by a rate that decreases from a maximum value λ_{max} to a minimum value λ_{min} in accordance with a simple time-decaying exponential function of time constant τ,

$$\lambda(t) = \lambda_{max}\exp(-t/\tau). \tag{33}$$

The probability density function $P(\lambda)$ is then distributed as $1/\lambda$ over an appropriate range of λ (Prucnal and Teich, 1983; Teich and Card, 1979), and, for an experiment of duration L, the mean and variance turn out to be:

$$\langle\lambda\rangle = \lambda_{max}(\tau/L)[1 - \exp(-L/\tau)] \tag{34}$$

and

$$\begin{aligned}\mathrm{Var}(\lambda) = \lambda_{max}^2\left(\frac{\tau}{L}\right)\Bigg[\left(\frac{1}{2} - \frac{\tau}{L}\right) + 2\left(\frac{\tau}{L}\right)\exp\left(-\frac{L}{\tau}\right) \\ - \left(\frac{1}{2} + \frac{\tau}{L}\right)\exp\left(-\frac{2L}{\tau}\right)\Bigg].\end{aligned} \tag{35}$$

Since $T \ll L$, Eq. (15) can be written as:

$$p(n,T) = \int_\lambda p(n,T|\lambda)\, P(\lambda)\, d\lambda, \tag{36}$$

so that all of the equations obtained thereafter can be considered as being conditioned on λ rather than on W. The unconditional Fano factor can then be obtained from Eq. (28) by using $F_{\lambda T}$ in place of F_W. A calculation of this type has been carried out earlier (Teich, 1989).

Acknowledgments

I am grateful to S. B. Lowen, R. G. Turcott, T. W. Woo, and N. Powers for useful discussions. This work was supported by the Joint Services Electronics Program and by the Office of Naval Research.

References

BARLOW, H. B., and LEVICK, W. R. (1969). "Changes in the Maintained Discharge with Adaptation Level in the Cat Retina," *Journal of Physiology (London)* **202,** 699–718.

CANTOR, B. I., and TEICH, M. C. (1975). "Dead-Time-Corrected Photocounting Distributions for Laser Radiation," *Journal of the Optical Society of America* **65,** 786–791.

M. C. Teich, "Fractal Neuronal Firing Patterns," in Single Neuron Computation, edited by T. McKenna, J. Davis, and S. F. Zornetzer (Academic Press, Boston, 1992), ch. 22, pp. 589-625

Cox, D. R. (1962). *Renewal Theory*. Methuen, London.

Cox, D. R., and Lewis, P. A. W. (1966). *The Statistical Analysis of Series of Events*. Methuen, London.

Fano, U. (1947). "Ionization Yield of Radiations. II. The Fluctuations of the Number of Ions," *Physical Review* **72,** 26–29.

Feller, W. (1951). "The Asymptotic Distribution of the Range of Sums of Independent Random Variables," *Annals of Mathematical Statistics* **22,** 427–432.

Gaumond, R. P., Molnar, C. E., and Kim, D. O. (1982). "Stimulus and Recovery Dependence of Cat Cochlear Nerve Fiber Spike Discharge Probability," *Journal of Neurophysiology* **48,** 856–873.

Gray, P. F. (1967). "Conditional Probability Analyses of the Spike Activity of Single Neurons," *Biophysical Journal* **7,** 759–777.

Harrison, R. V. (1985). "Long-Term Adaptation in Afferent Neurones from the Normal and Pathological Cochlea," *Journal of the Acoustical Society of America Supplement 1* **77,** S94.

Hurst, H. E. (1951). "Long-Term Storage Capacity of Reservoirs," *Transactions of the American Society of Civil Engineers* **116,** 770–808.

Khanna, S. M., and Teich, M. C. (1989a). "Spectral Characteristics of the Responses of Primary Auditory-Nerve Fibers to Amplitude-Modulated Signals," *Hearing Research* **39,** 143–158.

Khanna, S. M., and Teich, M. C. (1989b). "Spectral Characteristics of the Responses of Primary Auditory-Nerve Fibers to Frequency-Modulated Signals," *Hearing Research* **39,** 159–176.

Kuffler, S. W., FitzHugh, R., and Barlow, H. B. (1957). "Maintained Activity in the Cat's Retina in Light and Darkness," *Journal of General Physiology* **40,** 683–702.

Legéndy, C. R., and Salcman, M. (1985). "Bursts and Recurrences of Bursts in the Spike Trains of Spontaneously Active Striate Cortex Neurons," *Journal of Neurophysiology* **53,** 926–939.

Liebovitch, L. S., and Tóth, T. I. (1990). "Using Fractals to Understand the Opening and Closing of Ion Channels," *Annals of Biomedical Engineering* **18,** 177–194.

Lowen, S. B., and Teich, M. C. (1990). "Power-Law Shot Noise," *IEEE Transactions on Information Theory* **36,** 1302–1318.

Lowen, S. B., and Teich, M. C. (1991). "Doubly Stochastic Poisson Point Process Driven by Fractal Shot Noise," *Physical Review A* **43,** 4192–4215.

Lütkenhöner, B., and Smith, R. L. (1986). "Rapid Adaptation of Auditory-Nerve Fibers: Fine Structure at High Stimulus Intensities," *Hearing Research* **24,** 289–294.

Mandelbrot, B. B. (1983). *The Fractal Geometry of Nature*. Freeman, New York.

Matsuo, K., Saleh, B. E. A., and Teich, M. C. (1982). "Cascaded Poisson Processes," *Journal of Mathematical Physics* **23,** 2353–2364.

McGill, W. J., and Teich, M. C. (1991a). "Auditory Signal Detection and Amplification in a Neural Transmission Network," in M. L. Commons, J. A. Nevin, and M. C. Davison (eds.), *Signal Detection* (pp. 1–37). Lawrence Erlbaum, Hillsdale, New Jersey.

M. C. Teich, "Fractal Neuronal Firing Patterns," in Single Neuron Computation, edited by T. McKenna, J. Davis, and S. F. Zornetzer (Academic Press, Boston, 1992), ch. 22, pp. 589-625

McGILL, W. J., and TEICH, M. C. (1991b). *Simple Models of Sensory Transmission* (Report no. CHIP 132). Center for Human Information Processing, University of California (San Diego), La Jolla, California.

MUELLER, C. G. (1954). "A Quantitative Theory of Visual Excitation for the Single Photoreceptor," *Proceedings of the National Academy of Sciences* **40,** 853–863.

MÜLLER, J. W. (1974). "Some Formulae for a Dead-Time-Distorted Poisson Process," *Nuclear Instrumentation and Methods* **117,** 401–404.

POWERS, N. (1991). *Discharge Rate Fluctuations in the Auditory Nerve of the Chinchilla.* Unpublished Doctoral Dissertation. State University of New York at Buffalo.

POWERS, N. L., SALVI, R. J., and SAUNDERS, S. S. (1991). "Discharge Rate Fluctuations in the Auditory Nerve of the Chinchilla (Abstract no. 411)," in D. J. Lim (ed.), *Abstracts of the Fourteenth Midwinter Research Meeting of the Association for Research in Otolaryngology,* p. 129. Association for Research in Otolaryngology, Des Moines, Iowa.

PRUCNAL, P. R., and TEICH, M. C. (1979). "Statistical Properties of Counting Distributions for Intensity-Modulated Sources," *Journal of the Optical Society of America* **69,** 539–544.

PRUCNAL, P. R., and TEICH, M. C. (1983). "Refractory Effects in Neural Counting Processes with Exponentially Decaying Rates," *IEEE Transactions on Systems, Man and Cybernetics* **SMC-13,** 1028–1033.

RICCIARDI, L. M., and ESPOSITO, F. (1966). "On Some Distribution Functions for Non-Linear Switching Elements with Finite Dead Time," *Kybernetik (Biological Cybernetics)* **3,** 148–152.

SHOFNER, W. P., and DYE, R. H., JR. (1989). "Statistical and Receiver Operating Characteristic Analysis of Empirical Spike-Count Distributions: Quantifying the Ability of Cochlear Nucleus Units to Signal Intensity Changes," *Journal of the Acoustical Society of America* **86,** 2172–2184.

TEICH, M. C. (1981). "Role of the Doubly Stochastic Neyman Type-A and Thomas Counting Distributions in Photon Detection," *Applied Optics* **20,** 2457–2467.

TEICH, M. C. (1985). "Normalizing Transformations for Dead-Time-Modified Poisson Counting Distributions," *Biological Cybernetics* **53,** 121–124.

TEICH, M. C. (1989). "Fractal Character of the Auditory Neural Spike Train, *IEEE Transactions on Biomedical Engineering* **36,** 150–160.

TEICH, M. C., and CARD, H. C. (1979). "Photocounting Distributions for Exponentially Decaying Sources," *Optics Letters* **4,** 146–148.

TEICH, M. C., and DIAMENT, P. (1969). "Flat Counting Distribution for Triangularly Modulated Poisson Process," *Physics Letters* **30A,** 93–94.

TEICH, M. C., and DIAMENT, P. (1980). "Relative Refractoriness in Visual Information Processing," *Biological Cybernetics* **38,** 187–191.

TEICH, M. C., and KHANNA, S. M. (1985). "Pulse-Number Distribution for the Neural Spike Train in the Cat's Auditory Nerve," *Journal of the Acoustical Society of America* **77,** 1110–1128.

TEICH, M. C., and SALEH, B. E. A. (1988). "Photon Bunching and Antibunching," in E. Wolf (ed.), *Progress in Optics, Vol. 26* (pp. 1–104). Elsevier, Amsterdam.

M. C. Teich, "Fractal Neuronal Firing Patterns," in Single Neuron Computation, edited by T. McKenna, J. Davis, and S. F. Zornetzer (Academic Press, Boston, 1992), ch. 22, pp. 589-625

TEICH, M. C., and TURCOTT, R. G. (1988). "Multinomial Pulse-Number Distributions for Neural Spikes in Primary Auditory Fibers: Theory," *Biological Cybernetics* **59,** 91–102.

TEICH, M. C., LOWEN, S. B., and TURCOTT, R. G. (1991). "On Possible Peripheral Origins of the Fractal Auditory Neural Spike Train (Abstract no. 154)," in D. J. Lim (ed.), *Abstracts of the Fourteenth Midwinter Research Meeting of the Association for Research in Otolaryngology,* p. 50. Association for Research in Otolaryngology, Des Moines, Iowa.

TEICH, M. C., MATIN, L., and CANTOR, B. I. (1978). "Refractoriness in the Maintained Discharge of the Cat's Retinal Ganglion Cell," *Journal of the Optical Society of America* **68,** 386–402.

TEICH, M. C., TURCOTT, R. G., and LOWEN, S. B. (1990a). "The Fractal Doubly Stochastic Poisson Point Process as a Model for the Cochlear Neural Spike Train," in P. Dallos, C. D. Geisler, J. W. Matthews, M. A. Ruggero, and C. R. Steele (eds.), *The Mechanics and Biophysics of Hearing (Lecture Notes in Biomathematics, Vol. 87)* (pp. 354–361). Springer-Verlag, New York.

TEICH, M. C., JOHNSON, D. H., KUMAR, A. R., and TURCOTT, R. G. (1990b). "Rate Fluctuations and Fractional Power-Law Noise Recorded from Cells in the Lower Auditory Pathway of the Cat," *Hearing Research* **46,** 41–52.

TURCOTT, R. G., LOWEN, S. B., TEICH, M. C., JOHNSON, D. H., and TSUCHITANI, C. (1991). Personal communication.

VOSS, R. F., and CLARKE, J. (1978). " '1/*f* Noise' in Music: Music from 1/f Noise," *Journal of the Acoustical Society of America* **63,** 258–263.

WALSH, B. T., MILLER, J. B., GACEK, R. R., and KIANG, N. Y-S. (1972). "Spontaneous Activity in the Eighth Cranial Nerve of the Cat," *International Journal of Neuroscience* **3,** 221–236.

WOO, T. W. (1991). *Fractals in Auditory-Nerve Spike Trains.* Unpublished Master's Dissertation. Johns Hopkins University, Baltimore.

WOO, T. W., SACHS, M. B., and TEICH, M. C. (1992). "1/*f*-like Spectra in Cochlear Neural Spike Trains," in *Abstracts of the Fifteenth Midwinter Research Meeting of the Association for Research in Otolaryngology.* Association for Research in Otolaryngology, Des Moines, Iowa.

YOUNG, E. D., and BARTA, P. E. (1986). "Rate Responses of Auditory Nerve Fibers to Tones in Noise near Masked Threshold," *Journal of the Acoustical Society of America* **79,** 426–442.

M. C. Teich, "Fractal Neuronal Firing Patterns," in Single Neuron Computation, edited by T. McKenna, J. Davis, and S. F. Zornetzer (Academic Press, Boston, 1992), ch. 22, pp. 589-625